



A Journal of



Accepted Article

Title: 4,6-Diacetyl Resorcinol Based Vanadium(V) Complexes: Reactivity and Catalytic Applications

Authors: Mannar R. Maurya, Nancy Jangra, Fernando Avecilla, and Isabel Correia

This manuscript has been accepted after peer review and appears as an Accepted Article online prior to editing, proofing, and formal publication of the final Version of Record (VoR). This work is currently citable by using the Digital Object Identifier (DOI) given below. The VoR will be published online in Early View as soon as possible and may be different to this Accepted Article as a result of editing. Readers should obtain the VoR from the journal website shown below when it is published to ensure accuracy of information. The authors are responsible for the content of this Accepted Article.

To be cited as: *Eur. J. Inorg. Chem.* 10.1002/ejic.201801243

Link to VoR: <http://dx.doi.org/10.1002/ejic.201801243>

WILEY-VCH

4,6-Diacetyl Resorcinol Based Vanadium(V) Complexes: Reactivity and Catalytic Applications

Mannar R. Maurya,^{*[a]} Nancy Jangra,^[a] Fernando Avecilla^[b] and Isabel Correia^[c]

AUTHORS ADDRESS

[a] Prof. Dr. Mannar R. Maurya, Ms. Nancy Jangra

Department of Chemistry, Indian Institute of Technology Roorkee, Roorkee 247667, India

E-mail: rkmanfcy@iitr.ac.in; Fax: +91 1332 273560; Tel: +91 1332 285327;
<https://www.iitr.ac.in/CY/rkmanfcy>

[b] Prof. Dr. Fernando Avecilla

Grupo Xenomar, Centro de Investigacións Científicas Avanzadas (CICA), Departamento de Química, Facultade de Ciencias, Universidade da Coruña, Campus de A Coruña, 15071 A Coruña, Spain

[c] Dr. Isabel Correia

Centro de Química Estrutural, Instituto Superior Técnico, Universidade Lisboa, 1049-001 Lisboa, Portugal

Keywords: Vanadium complexes · Haloperoxidases models · Structure elucidation · Homogeneous catalysis · Oxidative bromination · Catalytic epoxidation of alkenes

Abstract: Four ONO donor ligands are isolated from the condensation of 4,6-diacetyl resorcinol with isonicotinoyl hydrazide (H₂dar-inh, **I**), nicotinoyl hydrazide (H₂dar-nah, **II**), benzoyl hydrazide (H₂dar-bhz, **III**) and 2-furoyl hydrazide (H₂dar-fah, **IV**) on refluxing in MeOH. The reaction of *in situ* generated aqueous K[H₂V^VO₄] with ligands **I-IV** at neutral pH gives complexes, [K(H₂O)₂][VO₂(dar-inh)] (**1**), [K(H₂O)₂][VO₂(dar-nah)] (**2**), [K(H₂O)₂][VO₂(dar-bhz)] (**3**) and [K(H₂O)₂][VO₂(dar-fah)] (**4**), respectively. The reaction of [V^{IV}O(acac)₂] (acac = acetylacetonato) with these ligands (**I-IV**) under aerobic conditions in methanol yields oxidomethoxovanadium(V) complexes, [VO(OMe)(MeOH)(dar-inh)] (**5**), [VO(OMe)(MeOH)(dar-nah)] (**6**), [VO(OMe)(MeOH)(dar-bhz)] (**7**) and [VO(OMe)(MeOH)(dar-fah)] (**8**). All the isolated complexes are characterized by elemental, thermal, electrochemical and spectroscopic techniques [FT-IR, UV-Vis, NMR (¹H, ¹³C and ⁵¹V

NMR)] and single crystal X-ray diffraction analysis (for **1**, **6**, **7** and **8**). X-ray analysis confirms the coordination of the ligands through O_{phenolate}, N_{azomethine} and O_{enolate} to the metal center. In the molecular structure of [K(H₂O)(EtOH)][V^VO₂(dar-inh)] (abbreviated as **1a** where one molecule of water is replaced by EtOH), water molecules act as bridges between two K⁺ ions and the complex shows a dimeric structure due to the presence of electrostatic interactions between V=O oxygen atoms with K⁺ ions. These complexes are active catalysts for the oxidative bromination of thymol in the presence of KBr, HClO₄ and H₂O₂ and give 2-bromothymol, 4-bromothymol and 2,4-dibromothymol as major products. Complexes **1-4** were also tested as catalysts for the epoxidation of various alkenes (namely styrene, cyclohexene, *cis*-cyclooctene, 1-hexene, 1-octene, cyclohexenone and trans-stilbene) with H₂O₂ in the presence of NaHCO₃ as promoter giving the corresponding epoxides selectively.

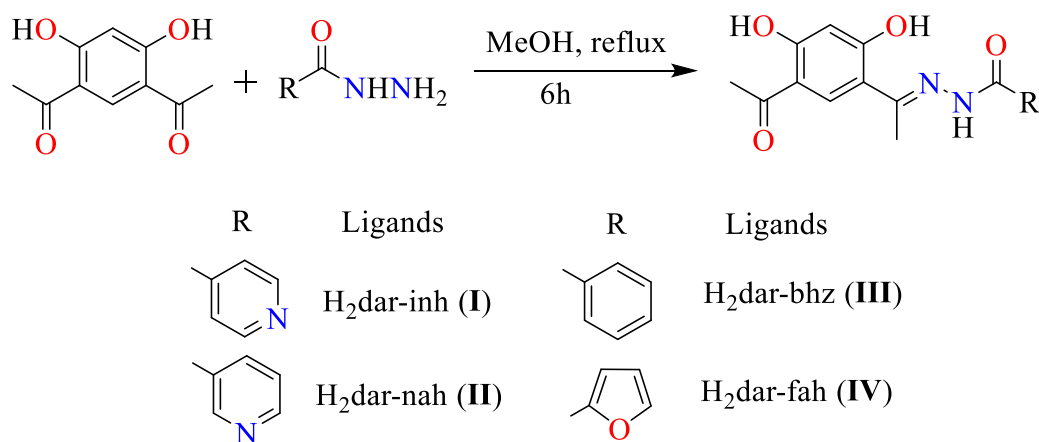
Introduction

A remarkable research growth on mononuclear oxidovanadium(V) complexes has been observed in recent decades due to interesting discoveries on vanadium bioinorganic chemistry.^[1] Biologically important compounds such as mononuclear oxidovanadium(V) complexes have also served as structural and functional models of vanadate-dependent haloperoxidases.^[2,3] These have also been explored as homogeneous catalysts for numerous catalytic transformations^[4] such as oxidative bromination,^[5] sulphoxidation,^[6] epoxidation of olefins,^[7] oxidation of alcohols,^[8] oxidation of aromatic hydrocarbons/cycloalkanes,^[9] hydroamination and oxidative amination,^[10] aromatization of 1,4-dihydropyridines,^[11] etc. Our research group has been actively engaged in the characterization of structural and functional models of haloperoxidases and has made efforts in exploring their catalytic potential towards some of the above transformations. Herein, we report the syntheses and characterization of dioxidovanadium(V) and oxidomethoxidovanadium(V) of ligands **I-IV** derived from 4,6-diacetyl resorcinol and various hydrazides, Scheme 1.

Difunctional 4,6-diacetyl resorcinol and its derivatives have attracted attention due to their biological and particularly pharmaceutical activity. Various hydrazones derived from 4,6-diacetyl resorcinol and their coordination complexes of nickel(II), cobalt(II), copper(II) and zinc(II) have been investigated against gram-negative (*Salmonella Typhi* and *Escherichia Coli*), and gram positive (*Bacillus Subtilis* and *Staphylococcus Aureus*) bacteria, as well as antifungal activity against *Candida Albicans*, *Aspergillus Niger* and *Cladosporium oxy-sporum*, with positive

results.^[12] In copper(II) complexes derived from the products of condensation of 4,6-diacetyl resorcinol with 3-hydrazino-5,6-diphenyl-1,2,4-triazine or isatin monohydrazone the antimicrobial activity of the ligands was enhanced by Cu-chelation.^[13]

Only a few reports have been made on the catalytic activity of 4,6-diacetyl resorcinol complexes. The activity of a copper(II) complex of a chitosan derivative showed high efficiency towards the decomposition of H₂O₂ as heterogeneous catalyst.^[14] Pd(II) complexes from Schiff bases derived from 4,6-diacetyl resorcinol provided high activity and substrate selectivity in the oxidation of 1-octene.^[15] Vanadium complexes of hydrazones of 4,6-diacetyl resorcinol have not yet been reported. Thus, we have explored the catalytic potential of vanadium complexes derived from the condensation of 4,6-diacetyl resorcinol with hydrazides towards the oxidative bromination of thymol (a monoterpene) and epoxidation of various alkenes (namely styrene, cyclohexene, *cis*-cyclooctene, 1-hexene, 1-octene, cyclohexanone and *trans*-stilbene).



Scheme 1. Synthetic scheme used to prepare ligands **I**, **II**, **III** and **IV** and their structural formulae.

Epoxidation reactions are extremely important transformations in organic chemistry since epoxides are key building blocks in organic synthesis^[16] and many vanadium complexes, such as VO(acac)₂ (acac = acetylacetonate) have been used to catalyse this reaction.^[17] However, there is still room for improvement. The catalytic halogenation of organic substrates, and particularly bromination reactions^[5] are very important as brominated compounds have interesting biological properties. The classical methods involving molecular bromine need to be replaced by safer and greener reactions.

Results and Discussion

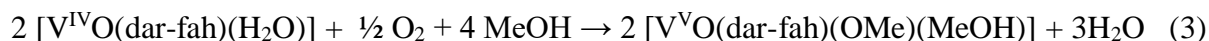
Synthesis and Solid-State Characterization of Complexes

Condensation of 4,6-diacetyl resorcinol with various hydrazides (Scheme 2) in equimolar ratio in MeOH resulted in the formation of the analytically pure ligands H₂dar-inh (**I**), H₂dar-nah (**II**), H₂dar-bhz (**III**) and H₂dar-fah (**IV**) in good yields (68-72% (Scheme 1).^[18] An aqueous solution of *in situ* generated potassium vanadate (predominantly K[H₂VO₄] at pH 7.0), obtained by dissolving V₂O₅ in aqueous KOH, reacted with the potassium salt of these ligands giving the potassium salts of the corresponding dioxidovanadium(V) anions [K(H₂O)₂][VO₂(dar-inh)] (**1**), [K(H₂O)₂][VO₂(dar-nah)] (**2**), [K(H₂O)₂][VO₂(dar-bhz)] (**3**) and [K(H₂O)₂][VO₂(dar-fah)] (**4**), respectively – see equation (1) considering **2** as a representative complex.



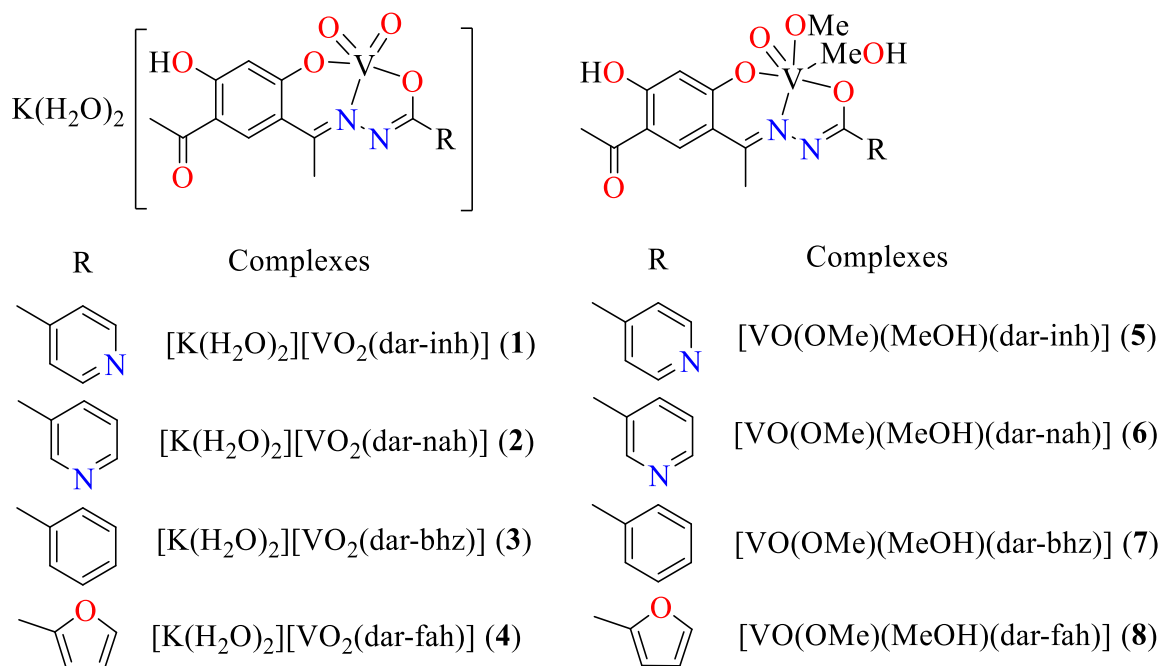
[V^{IV}O(acac)₂] (Hacac = acetylacetonate) also reacted with ligands **III** and **IV** in 1:1 molar ratio in methanol under reflux, followed by aerial oxidation to yield the mononuclear oxidomethoxidovanadium(V) complexes [VO(OMe)(MeOH)(dar-bhz)] (**7**) and [VO(OMe)(MeOH)(dar-fah)] (**8**), respectively. Equations (2) and (3) present a possible reaction sequence considering H₂dar-fah (**IV**) as a representative ligand.

Complexes [VO(OMe)(MeOH)(dar-inh)] (**5**) and [VO(OMe)(MeOH)(dar-nah)] (**6**) were obtained by aerial oxidation of complexes **1** and **2**, respectively, in methanol - equation (3). All V-complexes were obtained in moderate to good yields (68-85%).



For all complexes the molecular ion peak was found both in the positive and in the negative ionization mode. An overview of the complexes reported in this paper is presented in Scheme 2, based on elemental, thermal and electrochemical analyses and spectroscopic characterization data (ESI-MS, FT-IR, UV-Vis, ¹H and ¹³C NMR and ⁵¹V NMR).

Structures of complexes **1**, **6**, **7** and **8** have been further indorsed by single-crystal X-ray diffraction studies. These complexes exist as monomers and are soluble in MeOH, EtOH, CH₃CN, DMF, and DMSO, to different extents.



Scheme 2. Structural formulae of the complexes described in this work.

Thermal Studies

The thermal stability of the complexes was studied under oxygen atmosphere and relevant data and TGA profiles are presented in Table S1 and Figure S1. The profiles obtained for complexes **1-4** are consistent with i) the loss of one weakly coordinated water molecule; ii) the loss of L+H₂O-(O) moiety and iii) KVO₃ as the final product. Complexes **5-8** undergo mass losses roughly equivalent to i) one methanol molecule; ii) two overlapping steps equivalent to (OMe+L)-1.5O group, indicating the presence of a strongly coordinated methoxide group as well as the ligand and iii) V₂O₅ as the final product.

Description of Molecular Structures

ORTEP diagrams of **1a**, **6**, **7** and **8** are shown in Figures 1, 2, 3 and 4, respectively. Selected bond distances and angles are given in Tables 1 and 2. In all crystal structures coordination of the ligands to the metal center occurs through O_{phenolate}, N_{azomethine} and O_{enolate}.

Dihedral angles between the planes defined by the rings of the resorcinol moiety and the rings of hydrazides were measured in all structures. Angles of 5.69(22)° for **1a**, 12.26(12)° for **6**, 10.17(23)° for **7** and 13.39(17)° for **8** evidence the versatility of the ligands to adopt different conformations by rotation around the C(6)-C(9) bond, forming different atropoisomers.

Compound **1a** shows a dimeric structure due to the presence of electrostatic interactions between V=O oxygen atoms with K⁺ ions. Water molecules act as bridges between two K⁺ ions (see Figure 1). $\pi\cdots\pi$ stacking interactions are present in the structures in the crystal packing. The molecules are grouped in pairs through π - π interactions forming dimers in antiparallel positions (see Figure 4). The distance between centroids [c1, C(1H)-C(2H)-C(3H)-C(4H)-C(5H)-C(6H); c2, C(12B)-C(13B)-C(14B)-C(15B)-C(16B)-N(3AA)] is: $d_{c1-c2} = 3.758(3)$ Å for compound **1a**. In compound **6**, π -O interactions seem to be the governing factors and the molecules are grouped in intercalation positions through π - π interactions between R₂C-OH oxygen atoms and aromatic rings of the resorcinol moiety (see Figure S2). In **6** the distance between centroids [c5, C(1C)-C(2C)-C(3C)-C(4C)-C(5C)-C(6C), c6, O(4G)] is $d_{c5-c6} = 3.332(3)$ Å. Dihedral angles, ω , between the planes formed by the C=O groups and aromatic rings, can be used to determine if the close contacts between carbonyl oxygen atoms and aromatic centers correspond to lone-pair $\cdots\pi$ or $\pi\cdots\pi$ interactions.^[19] These angles are 3.4(2)°, close to 0°, indicating that they are $\pi\cdots\pi$ interactions.

The other two compounds present different crystal packing. The molecules are grouped in chains through π - π interactions between C=O groups of resorcinol moiety and phenyl rings and π - π interactions between rings of resorcinol groups (see Figures S3 and S4). The distances between centroids are: for **7**, $d_{c7-c8} = 3.651(2)$ Å for the centroids situated in resorcinol groups [c7, C(1C)-C(2C)-C(3C)-C(4C)-C(5C)-C(6C); c8, C(1N)-C(2N)-C(3N)-C(4N)-C(5N)-C(6N)] and $d_{c9-c10} = 3.265(2)$ Å for π -O interactions [c9, C(12A)-C(13A)-C(14A)-C(15A)-C(16A)-C(17A); c10, O(5K)]. Dihedral angles, ω , between the planes formed by the C=O groups and aromatic rings, are 5.4(2)°, for **8**, $d_{c11-c12} = 3.749(3)$ Å for the centroids situated in resorcinol groups [c11, C(1C)-C(2C)-C(3C)-C(4C)-C(5C)-C(6C); c12, C(1O)-C(2O)-C(3O)-C(4O)-C(5O)-C(6O)] and $d_{c13-c14} =$

3.303(3) Å for π -O interactions [c9, C(12B)-C(13B)-C(14B)-C(15B)-O(4B); c10, O(6M)]. Dihedral angles, ω , between the planes formed by the C=O groups and aromatic rings, 8.6(3)°, also close next to 0. Hydrogen bonding details of compounds **1a**, **6**, **7** and **8** are given in Table 3.

Table 1. Bond lengths [Å] and angles [°] for the compound **1a**.

Bond lengths		Bond angles	
V(1)-O(1)	1.605(4)	O(1)-V(1)-O(2)	107.71(19)
V(1)-O(2)	1.638(3)	O(1)-V(1)-O(4)	104.41(17)
V(1)-O(3)	1.958(3)	O(2)-V(1)-O(4)	93.29(15)
V(1)-O(4)	1.908(3)	O(1)-V(1)-O(3)	101.95(17)
V(1)-N(1)	2.149(4)	O(2)-V(1)-O(3)	94.37(15)
V(1)-K(1)	3.5488(15)	O(4)-V(1)-O(3)	148.78(16)
K(1)-O(6)#1	2.739(3)	O(1)-V(1)-N(1)	108.21(17)
K(1)-O(7)	2.786(4)	O(2)-V(1)-N(1)	143.92(18)
K(1)-O(8)	2.800(4)	O(4)-V(1)-N(1)	80.98(13)
K(1)-O(8)#2	2.862(4)	O(3)-V(1)-N(1)	75.10(12)
K(1)-O(1)	2.907(4)		
K(1)-O(2)	3.004(4)		
K(1)-O(7)#3	3.062(4)		

Table 2. Bond lengths [\AA] and angles [$^\circ$] for the compounds **6**, **7** and **8**.

Bond lengths	6	7	8
V(1)-O(1)	1.5785(19)	1.589(3)	1.5902(14)
V(1)-O(2)	1.9524(17)	1.856(3)	1.9484(14)
V(1)-O(3)	1.8652(17)	1.934(3)	1.8596(13)
V(1)-N(1)	2.139(2)	2.142(4)	2.1526(16)
V(1)-O(1S/M)	2.3597(19)	2.306(3)	2.3559(15)
V(1)-O(2S/M)	1.7718(18)	1.771(3)	1.7723(14)
Bond angles	6	7	8
O(1)-V(1)-O(2)	100.86(9)	100.29(14)	97.65(7)
O(1)-V(1)-O(3)	100.09(9)	98.95(13)	98.92(7)
O(2)-V(1)-O(3)	150.14(8)	151.76(12)	153.64(7)
O(1)-V(1)-N(1)	94.18(10)	94.10(14)	98.01(7)
O(2)-V(1)-N(1)	75.17(7)	82.76(12)	75.19(6)
O(3)-V(1)-N(1)	82.31(8)	75.42(12)	82.30(6)
O(1)-V(1)-O(2S/M)	101.69(10)	100.15(14)	101.52(8)
O(2S/M)-V(1)-O(2)	96.03(8)	103.18(12)	95.16(7)
O(2S/M)-V(1)-O(3)	100.29(8)	93.51(13)	101.41(6)
O(2S/M)-V(1)-N(1)	163.13(8)	163.22(13)	159.24(7)
O(1)-V(1)-O(1S/M)	175.56(9)	175.84(15)	176.87(7)
O(2S/M)-V(1)-O(1S/M)	81.78(8)	83.74(13)	81.57(6)
O(2)-V(1)-O(1S/M)	75.89(7)	77.27(13)	81.49(6)
O(3)-V(1)-O(1S/M)	81.87(8)	82.18(12)	80.85(6)
N(1)-V(1)-O(1S/M)	82.11(8)	82.29(13)	78.86(6)

#1 x,y+1,z #2 -x+1,-y+1,-z+1 #3 -x+2,-y+1,-z+1

Table 3. Hydrogen bonds in the compounds **1a**, **6**, **7** and **8**.

D-H...A	Compound	d(D-H)	d(H...A)	d(D...A)	<(DHA)
O(5)-H(5)...O(6)	1a	0.82	1.83	2.556(5)	146.2
O(7)-H(7O)...O(2)#1	1a	0.74	2.14	2.828(6)	156.9
O(8)-H(8OA)...N(3)#2	1a	0.97	1.95	2.916(5)	176.4
O(8)-H(8OB)...O(4)	1a	0.97	2.21	3.036(4)	142.8
O(1M)-H(1M)...N(3)#5	6	0.80(4)	2.07(4)	2.830(3)	160(4)
O(4)-H(4O)...O(5)	6	0.92(4)	1.78(4)	2.569(3)	143(3)
O(1S)-H(1S)...O(5)#6	7	0.67(4)	2.10(4)	2.762(5)	173(5)
O(4)-H(4O)...O(5)	7	0.72(5)	1.90(5)	2.574(5)	155(5)
O(1M)-H(1M)...O(6)#7	8	0.80(3)	1.99(3)	2.787(2)	175(3)
O(5)-H(5O)...O(6)	8	0.74(3)	1.84(3)	2.550(2)	161(3)

Symmetry transformations used to generate equivalent atoms:

#1 $-x+1, -y+1, -z+1$ #2 $x+1, y, z+1$ #3 $-x+1, -y+2, -z+1$ #4 $x, y-1, z-1$ #5 $x+1/2, -y+1/2, -z+2$

#6 $-x+1, -y, -z$ #7 $-x+1, -y+1, -z$

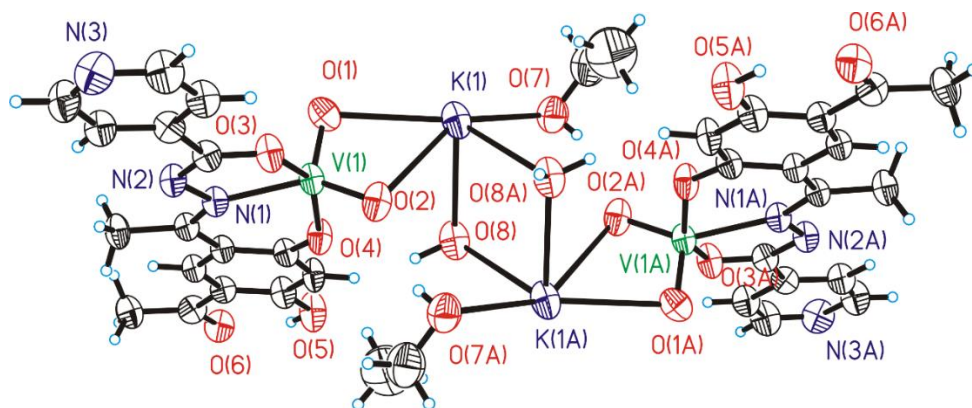


Figure 1. ORTEP plot for compound $[K(H_2O)(EtOH)][VO_2(dar-inh)]$ (**1a**). All the non-hydrogen atoms are presented by their 50% probability ellipsoids.

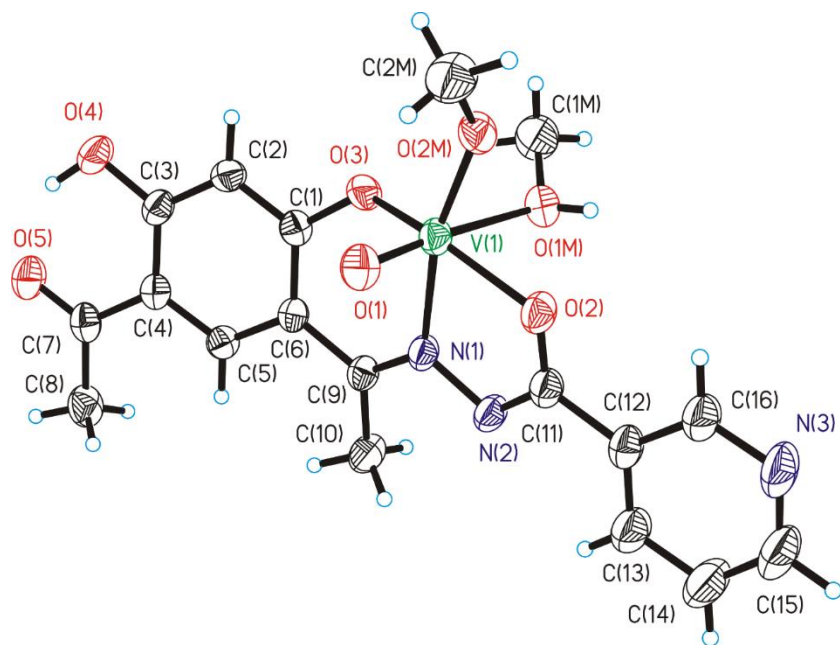


Figure 2. ORTEP plot for compound **6**. All the non-hydrogen atoms are presented by their 50% probability ellipsoids.

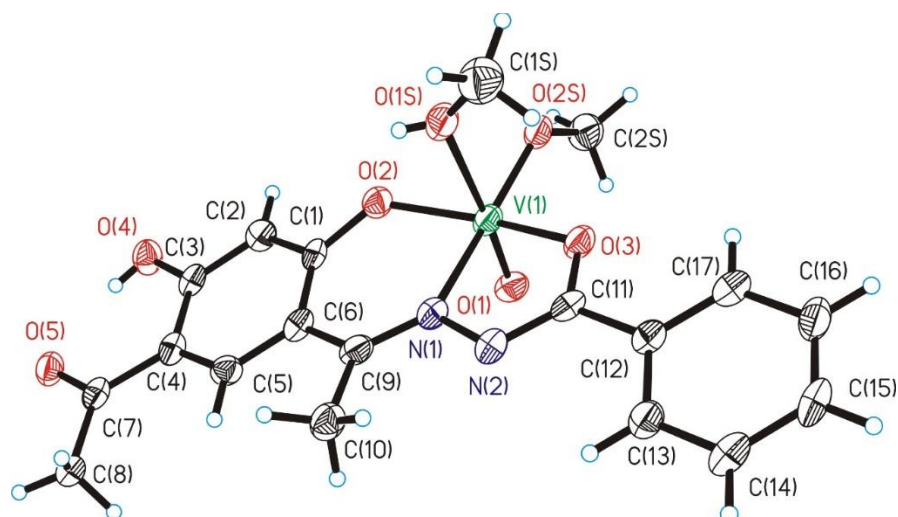


Figure 3. ORTEP plot for compound **7**. All the non-hydrogen atoms are presented by their 50% probability ellipsoids.

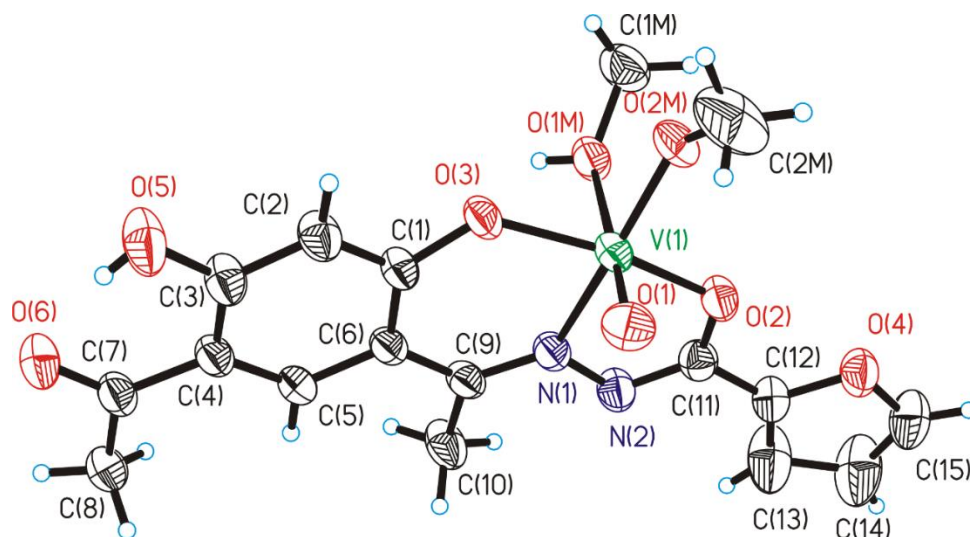


Figure 4. ORTEP plot for compound **8**. All the non-hydrogen atoms are presented by their 50% probability ellipsoids.

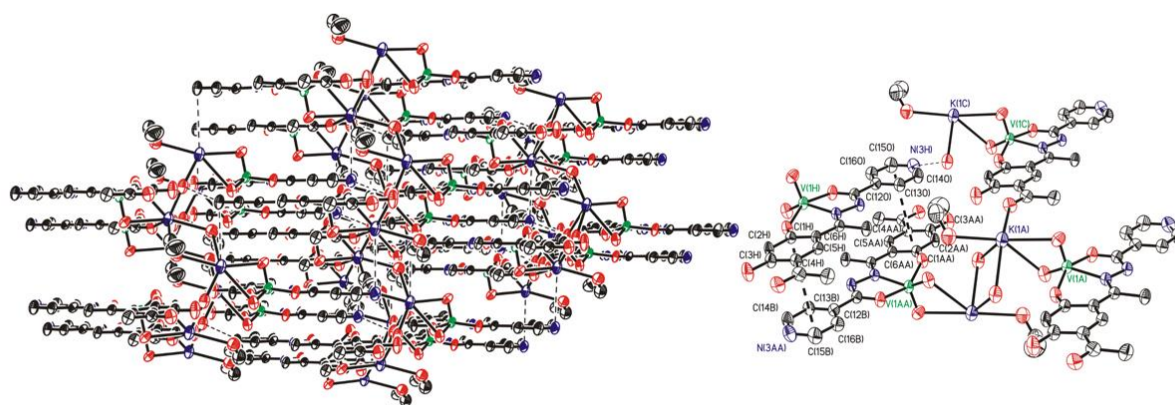


Figure 5. Crystal packing of compound **1** (left). The molecules are grouped in pairs through π - π interactions forming dimers in an antiparallel position (right). Drawings were done with SHELXL package.

IR Spectral Study

The details of IR spectral data of all ligands and their corresponding dioxidovanadium(V) anions and oxidomethoxidovanadium(V) complexes are given in Table S2. The characteristic bands in the spectra of ligands due to $\nu(\text{N-H})$ and $\nu(\text{C=O}_{\text{hydrazide}})$ appear in the range 3097-3129 and 1658-1687 cm^{-1} , respectively. These bands indicate a ketonic nature for the ligands in the free state. Disappearance of these bands in the spectra of the complexes and appearance of new bands in the region 1260-1280 cm^{-1} indicates enolization followed by coordination to the metal center after deprotonation. A strong band displayed by the ligands in the region 1561-1592 cm^{-1} is likely associated with $\nu(\text{C=N})$ stretching and this band shifts to lower wavenumbers in the spectra of the complexes, indicating coordination through the azomethine nitrogen. $[\text{V}^{\text{V}}\text{O}_2]^+$ complexes are characterized by the presence two sharp peaks in the region 884-940 cm^{-1} due to symmetric and antisymmetric $\nu(\text{O=V=O})$ stretching frequencies. A sharp band in the range 938-975 cm^{-1} is assigned to V=O stretching frequency of the $[\text{V}^{\text{V}}\text{O}]^{3+}$ complexes. The ligand band assigned to $\nu(\text{N-N})$ appearing at 936-988 cm^{-1} shows a bathochromic shift in the spectra of the complexes which further reinforces the assignment of the azomethine coordination. The broad band appearing at *ca.* 3086-3436 cm^{-1} in the spectra of the complexes is possibly due $\text{H}_2\text{O}/\text{MeOH}$ associated with the complexes as well as phenolic-OH groups, which were also present in the ligands' spectra at *ca.* 3267-3448 cm^{-1} .

UV-Vis Spectroscopic Studies

UV-vis spectral data (absorption maxima and respective extinction coefficients) of ligands and complexes are given in Table S3. Spectral studies of these ligands have been reported by us earlier ^[18] and spectra of the complexes are presented in Figure 6. The transitions $\varphi \rightarrow \varphi^*$, $\pi \rightarrow \pi^*$ and $n \rightarrow \pi^*$ show slight variations upon coordination to vanadium due to rearrangement and electronic donation of the ligands. Additionally, the complexes' spectra exhibit a new broad band of low intensity at 400-472 nm, which is assigned to ligand to metal charge transfer transition (LMCT), due to transfer of electron density from filled p-orbital of coordinated phenolate oxygen atoms to vacant d-orbitals of d^0 vanadium metal. The molar extinction coefficient of these bands (10^2 - 10^3) further reinforces the LMCT character. All the vanadium complexes are in d^0 state, hence no d-d transitions are expected.

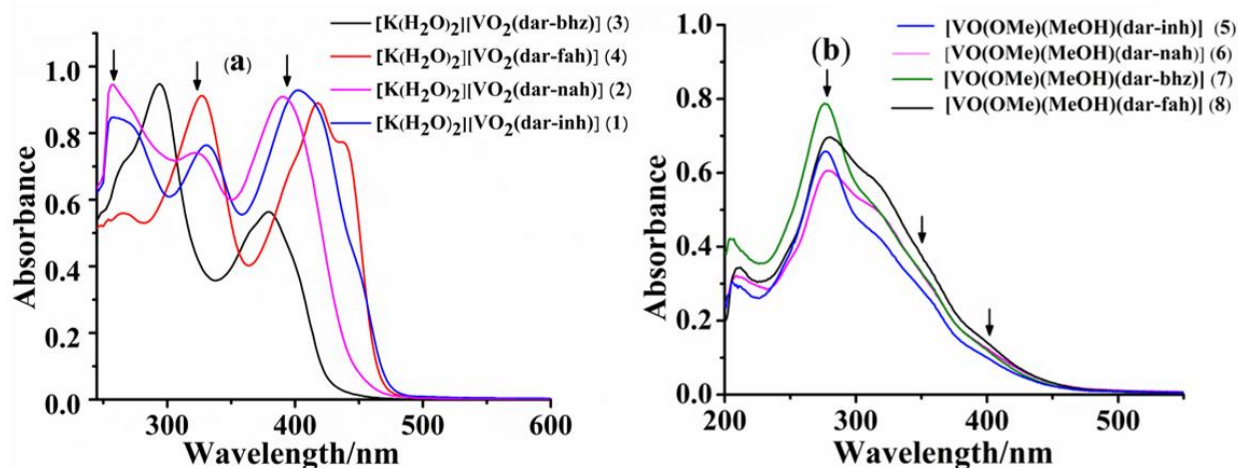


Figure 6. UV-Vis spectra of (a): dioxidovanadium(V) complexes **1-4** (2.30×10^{-4} M) and (b): oxidomethoxido vanadium (V) complexes **5** (2.71×10^{-5} M), **6** (3.47×10^{-5} M), **7** (2.70×10^{-5} M) and **8** (4.60×10^{-5} M) recorded in MeOH.

^1H and ^{13}C NMR Spectroscopic Studies

Further evidence for the coordination modes of the ligands and their corresponding $\text{V}^{\text{VO}}/\text{V}^{\text{VO}_2}$ complexes was obtained from ^1H NMR spectral studies. The relevant spectroscopic data of free ligands and their respective complexes, recorded in DMSO-d_6 are presented in Table 4, along with the values of coupling constants for aromatic protons. Representative spectra of ligand $\text{H}_2\text{dar-bhz}$ (**III**) and its complex $[\text{K}(\text{H}_2\text{O})_2][\text{VO}_2(\text{dar-bhz})]$ (**3**) are presented in Figure 7. In the ^1H NMR spectra of the ligands, two distinguishable singlets between $\delta = 12\text{--}14$ ppm show the presence of two phenolic protons in different environments. Disappearance of one of these signals confirms the coordination of only one phenolate oxygen atom to the vanadium ion after deprotonation; the other $-\text{OH}$ group remains uncoordinated. The spectra of all the ligands exhibit signals in the range $\delta = 11.18\text{--}11.63$ ppm due to the presence of $-\text{NH}$ protons while in the complexes these disappear, suggesting the enolization of the CO group of the hydrazide moiety and its coordination to vanadium. Signals due to methyl groups of coordinated methanol/methoxide appear at ca. $\delta = 3.1$ ppm. Overall, resonances due to aromatic and methyl protons of ligands and complexes appear in the expected regions with slight shifts in their positions.

Table 4. ^1H NMR data (δ in ppm) of ligands and complexes

Compound ^[a]	-OH	-NH	Aromatic Protons	Methyl Protons
H ₂ dar-inh (I)	14.34 (s, 1H), 12.62 (s, 1H)	11.63(s, 1H)	8.79 (d, $J = 5.2$ Hz, 2H), 8.11 (s, 1H), 7.84 (d, $J = 5.7$ Hz, 2H), 6.37 (s, 1H),	2.65 (s, 3H), 2.54 (s, 3H)
[K(H ₂ O) ₂][VO ₂ (dar-inh)] (1)	12.50 (s, 1H)	-	8.69 (d, $J = 2.2$ Hz, 2H), 8.33 (s, 1H), 7.90 (d, $J = 5.3$ Hz, 2H), 6.18 (s, 1H)	2.08 (s, 3H), 2.67 (s, 3H)
H ₂ dar-nah (II)	12.62 (br, 1H), 14.25 (br, 1H)	11.59(s, 1H)	9.08 (s, 1H), 8.7 (s, 1H), 8.27 (s, 1H), 8.16 (s, 1H), 7.57 (s, 1H), 6.38 (s, 1H)	2.66 (s, 3H), 2.56 (s, 3H)
[K(H ₂ O) ₂][VO ₂ (dar-nah)] (2)	12.50 (s, 1H)	-	9.17 (s, 1H), 8.67 (s, 1H), 8.31 (s, 2H), 7.50 (d, $J = 12.0$ Hz, 1H), 6.17 (s, 1H)	2.66 (s, 3H), 2.93 (s, 3H)
H ₂ dar-bhz (III)	12.65 (br, 1H), 14.50 (br, 1H)	11.41(s, 1H)	8.12 (s, 1H), 7.94 (d, $J=6.7$, 2H), 7.62 (t, $J=6.7$, 1H), 7.55 (t, $J=7.2$, 2H), 6.37 (s, 1H)	2.66 (s, 3H), 2.55 (s, 3H)
[K(H ₂ O) ₂][VO ₂ (dar-bhz)] (3)	12.50 (s, 1H)	-	8.30 (s, 1H), 6.16 (s, 1H), 8.03 (d, $J=5.9$, 2H), 7.45 (m, 3H)	2.93 (s, 3H), 2.66 (s, 3H)
H ₂ dar-fah (IV)	12.64 (br, 1H), 14.31 (br, 1H)	11.18(s, 1H)	8.11 (s, 1H), 7.80 (s, 1H), 7.42 (s, 1H), 6.74 (s, 1H), 6.36 (s, 1H)	2.66 (s, 3H), 2.52 (s, 3H)
[K(H ₂ O) ₂][VO ₂ (dar-fah)] (4)	12.51 (s, 1H)	-	6.07 (s, 1H), 8.12 (s, 1H), 7.80 (s, 1H), 6.62 (s, 1H), 6.97 (d, $J = 3.1$ Hz, 1H), 6.61 (d, $J = 1.5$ Hz, 1H)	2.86 (s, 3H), 2.54 (s, 3H)
H ₂ dhap-inh (V)	13.36 (br, 1H), 9.98 (s, 1H)	11.40(s, 1H)	8.77 (d, $J = 4.6$ Hz, 2H), 7.81 (d, $J = 5.7$ Hz, 2H), 7.47 (d, $J = 8.7$ Hz, 1H), 6.35 (d, $J = 8.7$ Hz, 1H), 6.29 (s, 1H),	2.39 (s, 1H)
[VO(OMe)(MeOH)(dar-inh)] (5)	12.52 (s, 1H)	-	6.26 (s, 1H), 8.38 (s, 1H), 8.86 (d, $J = 5.2$ Hz, 2H), 8.22 (d, $J = 5.2$ Hz, 2H),	2.69 (s, 3H), 2.96 (s, 3H)
[VO(OMe)(MeOH)(dar-nah)] (6)	12.53 (s, 1H)	-	6.18 (s, 1H), 9.18 (s, 1H), 8.67 (s, 1H), 8.32 (s, 2H), 7.50 (dd, $J = 7.0, 4.9$ Hz, 1H)	2.67 (s, 3H), 2.93 (s, 3H)
[VO(OMe)(MeOH)(dar-bhz)] (7)	12.58 (br, 1H)	-	8.37 (s, 1H), 6.39 (s, 1H), 8.06 (d, $J = 7.9$ Hz, 2H), 7.52 (m, 3H)	2.67 (s,3H), 2.9 0(s, 3H)
[VO(OMe)(MeOH)(dar-fah)] (8)	12.58 (br, 1H)	-	8.35 (s, 1H), 6.38 (s, 1H), 7.90 (s, 1H), 7.13 (d, $J = 3.4$ Hz, 1H), 6.68 (d, $J = 3.3$ Hz, 1H),	2.84 (s, 3H), 2.70 (s, 3H)

[a] Signals due to the methoxy protons in the spectra of the oxidovanadium (V) complexes: [VO(OMe)(MeOH)(dar-inh)] (**5**) at 3.17 ppm, [VO(OMe)(MeOH)(dar-nah)] (**6**) at 3.12 ppm, [VO(OMe)(MeOH)(dar-bhz)] (**7**) 3.21 ppm and [VO(OMe)(MeOH)(dar-fah)] (**8**) at 3.20 ppm were identified.

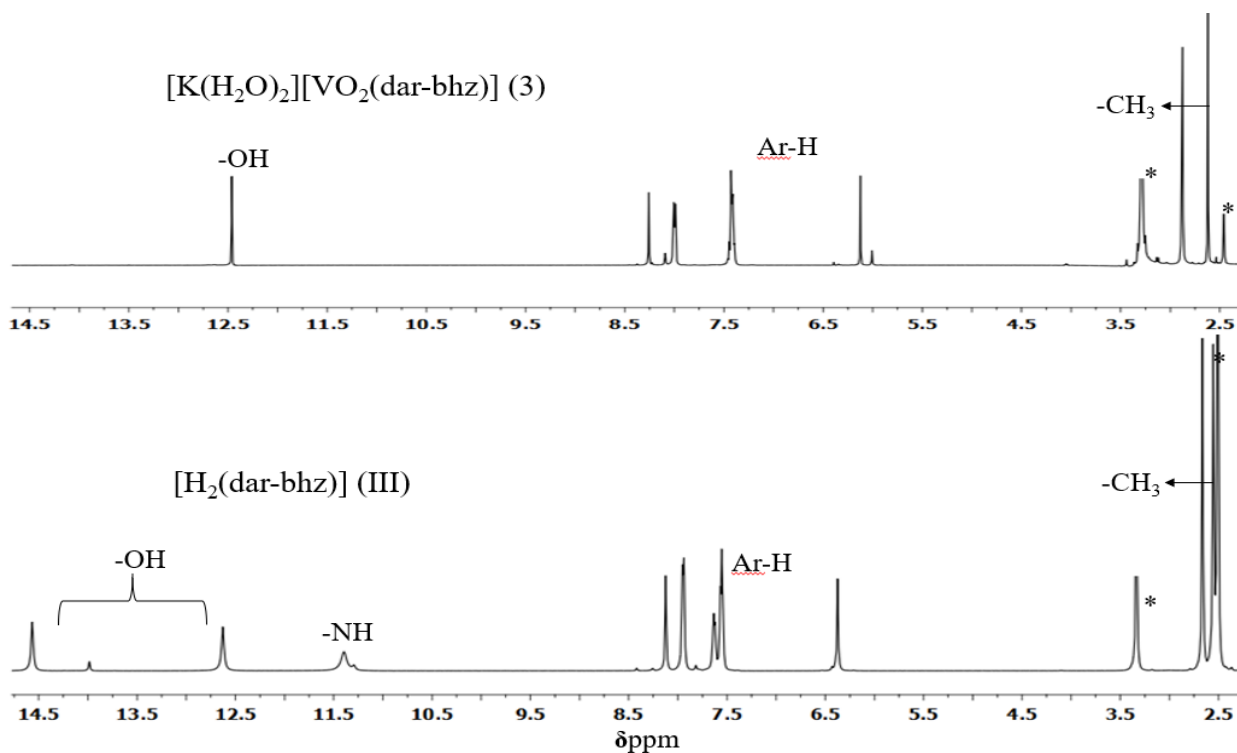


Figure 7. ¹H NMR spectra of ligand **III** and complex **3** recorded in DMSO-d₆. * indicates the proton impurity signal present in DMSO-d₆ at $\delta = 2.5$ ppm and that of moisture at $\delta = 3.25$ ppm.

The coordination modes of the ligands were further endorsed by ¹³C NMR studies. Table 5 reveals the complete details of ¹³C NMR chemical shift values of each carbon atom of ligands and respective complexes. Figure 8 depicts representative spectra of ligand H₂dar-fah (**IV**) and complex $[VO(OMe)(MeOH)(dar-fah)]$ (**8**). A significant chemical shift variation, $\Delta\delta = [\delta(\text{complex}) - \delta(\text{ligand})]$, was noticed in the signals of the carbon atoms which are present in the vicinity of the coordinating atoms O, N and O [i.e. phenolic oxygen (C3), azomethine nitrogen (C1) and enolic oxygen atom (C11)] assuring the coordination of O_{phenolate}, N_{azomethine} and O_{enolate} to the vanadium.^[20] Signals due to other carbon atoms of phenyl ring and methyl groups were observed in the expected δ values for the ligands as well as complexes, with slight variations, possibly due to electronic rearrangements. In addition, a new signal was observed in the spectra of complexes **5-8** at *ca.* $\delta = 49$ ppm, due to coordinated methoxy carbon atoms.

Table 5. ^{13}C NMR spectroscopic data (δ in ppm) of ligands and complexes

Compounds	C9	C1	C3	C11	Other carbons	C8	C10
H ₂ dar-inh (I)	203.56	166.43	164.43	163.32	164.98 (C5), 150.91 (C14/14'), 141.19 (C12), 134.55 (C7), 122.58 (C13/13'), 113.86 (C6), 113.09 (C2), 104.44 (C4)	14.81	27.36
[K(H ₂ O) ₂][VO ₂ (dar-inh)] (1) ($\Delta\delta$)	203.55	166.99 (0.56)	165.44 (1.01)	164.53 (1.21)	165.44 (C5), 150.47 (C14), 142.75 (C12), 136.35 (C7), 122.35 (C13), 114.96 (C6), 112.77 (C2), 105.78 (C4)	16.26	27.30
H ₂ dar-nah (II)	203.01	165.99	164.89	163.96	164.24 (C5), 158.32 (C16), 152.46 (C15), 149.0 (C13), 137.99 (C7), 12.89 (C12), 128.75 (C14), 123.59 (C6), 113.27 (C2), 112.64 (C4)	12.58	26.24
[K(H ₂ O) ₂][VO ₂ (dar-nah)] (2) ($\Delta\delta$)	202.86	171.28 (5.29)	166.92 (2.03)	165.27 (1.31)	163.48 (C5), 151.54 (C16), 149.40 (C15), 136.34 (C13), 135.75 (C7), 129.26 (C12), 124.06 (C14), 116.65 (C6), 113.18 (C2), 105.90 (C4)	16.13	27.65
H ₂ dar-bhz (III)	203.18	165.98	164.32	162.87	164.45 (C5), 133.52 (C12), 132.82 (C15), 128.49 (C7), 128.19 (C14/C16), 118.71, (C13/C17), 113.20 (C6), 112.80 (C2), 103.83 (C4)	13.91	27.47
[K(H ₂ O) ₂][VO ₂ (dar-bhz)] (3) ($\Delta\delta$)	203.00	171.19 (5.21)	168.47 (4.15)	165.14 (2.27)	164.84 (C5), 136.14 (C12), 133.64 (C15), 131.02 (C7), 128.70 (C14/C16), 128.25 (C13/C17), 116.82 (C6), 113.02(C2), 105.97 (C4)	16.22	27.42
H ₂ dar-fah (IV)	203.15	164.96	163.46	163.03	164.72 (C5), 155.65 (C12), 145.36 (C15), 140.39 (C7), 137.13 (C6), 133.39 (C13), 123.08 (C14), 113.65 (C2), 112.36 (C4)	13.88	27.81
[K(H ₂ O) ₂][VO ₂ (dar-fah)] (4) ($\Delta\delta$)	203.44	168.28	163.20	161.61	148.32 (C5), 145.66 (C12), 146.17 (C15), 136.20 (C7), 133.49 (C6), 115.86 (C13), 113.82 (C14), 112.39 (C2), 107.59(C4)	16.69	27.25

		(3.32)	(-0.26)	(-1.42)			
H ₂ dhap-inh (V)	-	163.15	161.13	161.36	160.98 (C5), 150.65 (C14), 140.34 (C12), 130.78 (C7), 122.02 (C13), 112.10 (C2), 107.75 (C6), 103.77 (C4)	14.56	-
[VO(OMe)(MeOH)(dar- inh)] (5)	202.13 (-1.4)	166.82 (0.39)	164.52 (0.09)	165.35 (2.03)	150.51 (C5), 136.66 (C14), 132.47 (C12), 136.66 (C7), 122.22 (C13), 116.88 (C6), 113.50 (C2), 105.84 (C4)	16.28	27.27
[VO(OMe)(MeOH)(dar- nah)] (6)	203.25 (3.9)	169.89 (2.02)	166.91 (2.02)	165.25 (1.29)	163.58 (C5), 151.51 (C16), 149.20 (C15), 136.34 (C13), 135.66 (C7), 124.08 (C12), 116.98 (C14), 114.78 (C6), 113.20 (C2), 106.02 (C4)	16.69	27.72
[VO(OMe)(MeOH)(dar- bhz)] (7)	202.45 (4.94)	170.92 (3.41)	167.73 (3.41)	164.84 (1.97)	161.63(C5), 136.87 (C12), 136.14 (C15), 133.64 (C7), 130.70 (C14/C16), 128.25 (C13/C17), 116.00 (C6), 113.02 (C2), 106.10 (C4)	17.84	28.45
[VO(OMe)(MeOH)(dar- fah)] (8)	203.31 (4.37)	169.33 (2.39)	165.85 (2.39)	162.24 (-0.79)	159.61 (C5), 146.42 (C12), 146.18 (C15), 136.13 (C7) 116.85 (C6), 115.38 (C13), 114.99 (C14), 112.67 (C2), 103.61 (C4)	17.07	27.83

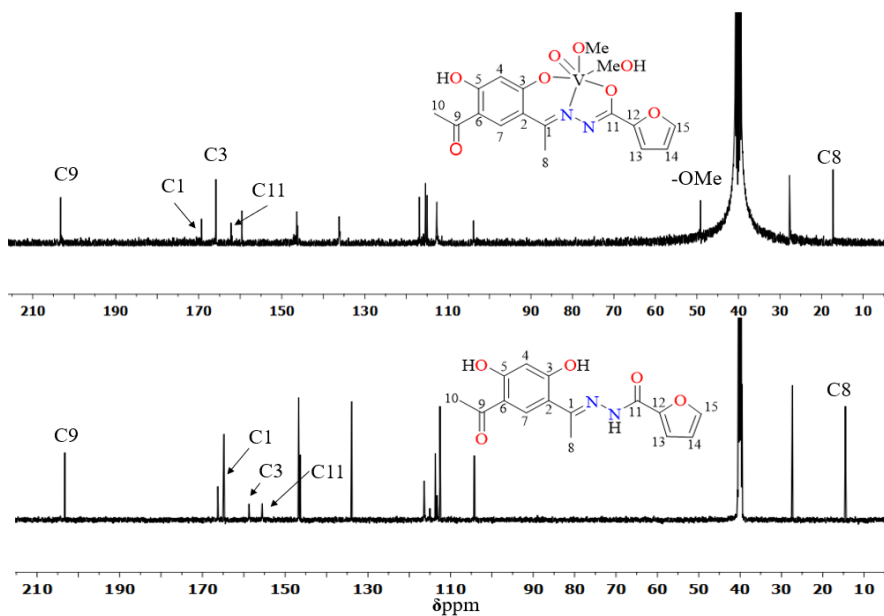


Figure 8. ¹³C NMR spectra of H₂dar(fah) (**IV**) and its vanadium complex [VO(OMe)(MeOH)(dar-fah)] (**8**) recorded in [DMSO]-d₆.

⁵¹V NMR Spectroscopic Study

Solutions for ⁵¹V NMR were prepared in MeOH and DMSO. Figure 9 shows the ⁵¹V NMR spectra measured for all complexes and Table 6 collects spectral bands. All complexes, except **4** in MeOH and **8** in DMSO, show the presence of only one peak with δ_V values between -533.7 and -547.8 ppm. In MeOH complex **4** shows two overlapped peaks at -546.5 and -547.75 ppm, while **8** in DMSO shows two peaks with ratios of 1:4 at -534.0 and -547.3 ppm, respectively. These chemical shifts are upfield from the ones found for the 4-benzoyl-3-methyl-1-phenyl-2-pyrazoline-5-one vanadium complexes,^[11] implying that the electronic density in the metal center is lower in this case, which is in agreement with the involvement of the phenolate donor.

Regarding the different substituents, in MeOH the order is from downfield to upfield: bhz < nah = inh < fah. The compounds with the benzene substituent appear more downfield and the ones containing the furane ring upfield, as expected due to electronic effects. However, in DMSO this does not happen and even complexes **5** and **6** have rather different chemical shifts (as well as the VO₂ complexes derived from nah and inh, **1** and **2**).

Table 6. Chemical shift of the peaks found in the ⁵¹V NMR spectra of vanadium complexes in MeOH and DMSO containing 10% of deuterated solvent.

Compound	MeOH	DMSO
[K(H ₂ O) ₂][VO ₂ (dar-inh)] (1)	-543.8	-533.7
[K(H ₂ O) ₂][VO ₂ (dar-nah)] (2)	-544.1	-536.6
[K(H ₂ O) ₂][VO ₂ (dar-bhz)] (3)	-536.8	-536.6
[K(H ₂ O) ₂][VO ₂ (dar-fah)] (4)	$-546.5, -547.8$	-538.0
[VO(OMe)(MeOH)(dar-inh)] (5)	-544.1	-536.7
[VO(OMe)(MeOH)(dar-nah)] (6)	-544.4	-544.6
[VO(OMe)(MeOH)(dar-bhz)] (7)	-540.9	-545.1
[VO(OMe)(MeOH)(dar-fah)] (8)	-545.9	$-534.0, -547.3$

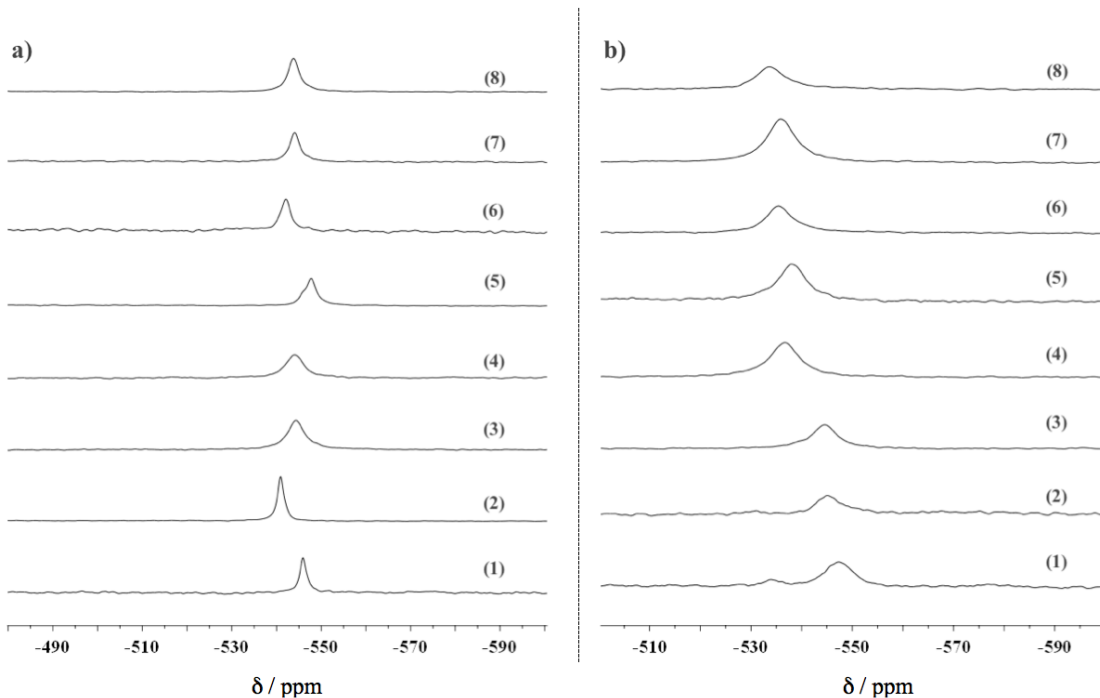


Figure 9. ^{51}V NMR spectra measured for solutions of the complexes dissolved in (a) MeOH containing 10% MeOD and b) DMSO containing 10% DMSO- d_6 .

Electrochemical Study

The electrochemical responses of all the ligands and complexes have been studied by measuring cyclic voltammograms (CV) in dry DMF, in order to investigate the redox stability of the complexes. Cyclic voltammograms of redox active ligands (**I-IV**) as well as complexes (**1-8**) were recorded in the range of 2.0 V to -2.0 V vs. SCE at room temperature and the CV results are given in Tables S4 and S5. As a representative example, the cyclic voltammograms of ligand H₂dar-bhz (**III**) and its complex [K(H₂O)₂][VO₂(dar-bhz)] (**3**) are shown in Figure 10 (for others see Figure S5). All the ligands exhibit one peak at ca. +1.0 V, which has been attributed to hydrazine-based ligand oxidation.^[21] Furthermore, in the cyclic voltammograms of all the complexes, a reductive response at ca. -0.8 V could be related to V(V) \rightarrow V(IV) reduction.^[22] This reductive response observed in the spectra of all the complexes is irreversible in nature. No further reduction responses were observed in any voltammogram of the complexes. Additionally, one oxidation peak in the potential window 1.09 -1.24 V is also observed in all the complexes which could be attributed to V(IV) \rightarrow V(V) oxidation.^[23] All vanadium complexes (**1-8**) showed identical redox processes,

which confirm similar structures and electronic features of the synthesized complexes. All these redox processes were also supported by DPV (see Tables S4 and S5).

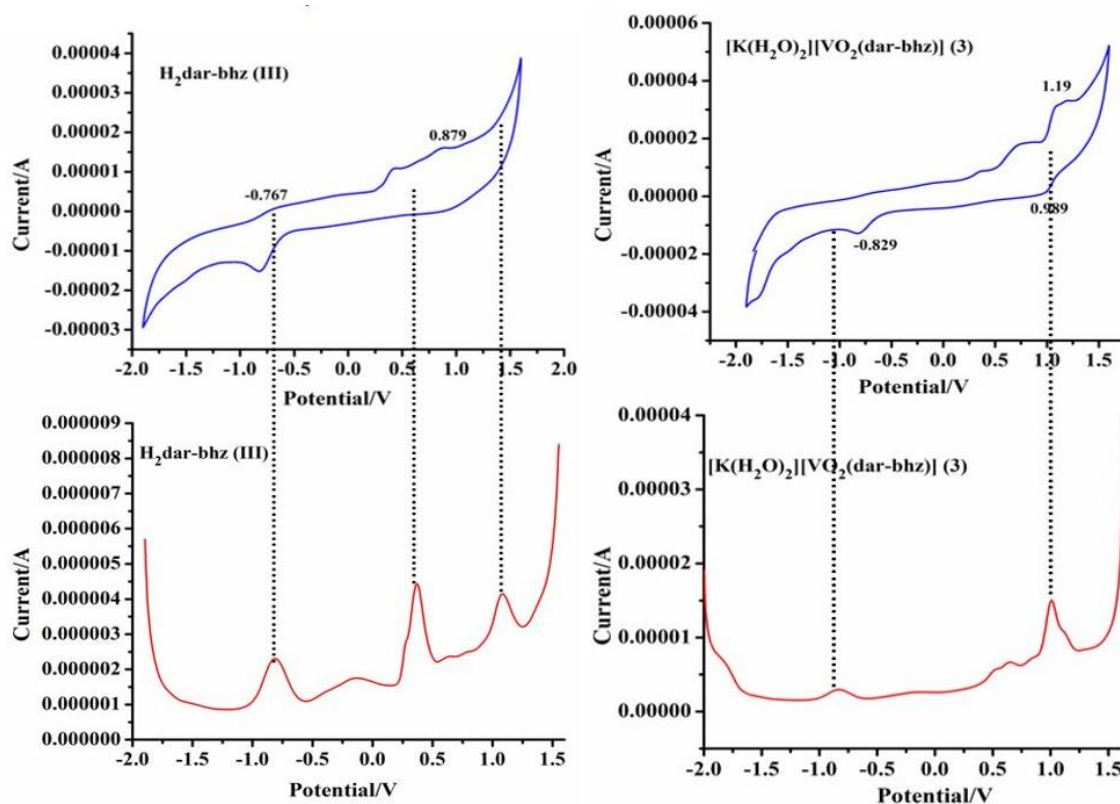
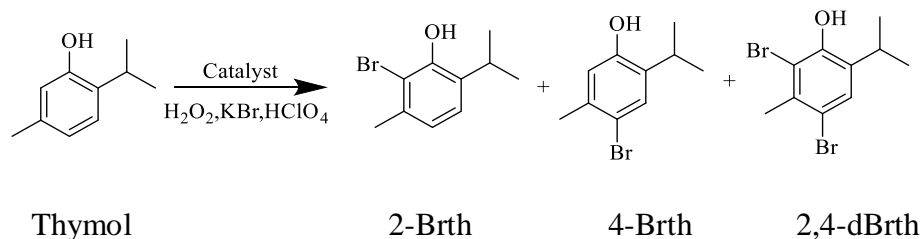


Figure 10. Comparative study of cyclic voltammograms and differential pulse voltammetry for $\text{H}_2\text{dar-bhz (III)}$ and $[\text{K}(\text{H}_2\text{O})_2][\text{VO}_2(\text{dar-bhz})] \text{ (3)}$ at a scan rate of 100 mV/s recorded in absolute dry DMF in the range 2.0 V to -2.0 V vs. Ag/AgCl at 298 K with 0.1 M TBAPF₆ as a supporting electrolyte.

Catalytic Studies

Oxidative Bromination of Thymol: The oxidative bromination of thymol was carried out in the presence of KBr, 70 % aqueous HClO_4 , and 30 % aqueous H_2O_2 in aqueous medium. The catalytic reaction led to the formation of three products, namely, 2-bromothymol, 4-bromothymol and 2,4-dibromothymol.^[24] Among these products 2,4-dibromothymol is formed due to further bromination of monobrominated products. The reaction takes place on the most activated site as a result of electrophilic aromatic substitution in the phenolic ring.



Scheme 3. Products of the oxidative bromination of thymol (2-Brth = 2-bromothymol, 4-Brth = 4-bromothymol, 2,4-dBrth = 2,4-dibromothymol).

Further, to obtain the maximum yield of brominated products, several parameters were changed, such as the amount of catalyst, KBr, H_2O_2 and HClO_4 using **3** as a representative catalyst. The conversion of thymol obtained in the different assays and the selectivity for the different brominated products, under particular conditions, are summarized in Table 7 and Figure S6 presents time-conversion plots obtained different conditions. It is clear from the data shown in Table 7 that the conversion and the selectivity for the products differ on varying the reagents. Thus, reaction conditions presented in entry 5 are suitable for obtaining the highest selectivity for 4-bromothymol (*ca.* 90%) while conditions in entry 9 are suitable for the highest selectivity of 2,4-dibromothymol (*ca.* 84%). However, the best reaction conditions for the maximum oxidative conversion (98 % conversion) of thymol with minimum amount of different reagents are: catalyst (0.001 g, 2.1×10^{-3} mmol), H_2O_2 (1.1 g, 10 mmol), KBr (1.2 g, 10 mol), and HClO_4 (1.2 g, 10 mol) in 20 mL water (Entry 1 of Table 7). Under these conditions, the selectivity observed follows the order 2,4-dibromothymol (49%) > 4-bromothymol (46%) > 2-bromothymol (5%).

The other three catalysts, *i.e.* complexes **1**, **2** and **4** were also tested under the above reaction conditions for the maximum conversion of thymol in 2 h of reaction time and the results are summarized in Table 8. The catalytic potential of these complexes compares well with results obtained with other metal complexes, such as: $[\text{V}^{\text{V}}\text{O}(\text{acac})(6,6'-(2-(\text{pyridin-2-yl})\text{ethylazanediyl})\text{bis}(\text{methylene})\text{-bis}(2,4\text{-di-tertbutylphenol}))]$,^[5e] $\text{Cs}(\text{H}_2\text{O})[\text{V}^{\text{V}}\text{O}_2(3,5\text{-bis}(2\text{-hydroxyphenyl})\text{-1-phenyl-1,2,4-triazole})]$ ^[5b] and $[\text{Mo}^{\text{VI}}\text{O}_2(8\text{-formyl-7-hydroxy-4-methylcoumarin-bhz})(\text{MeOH})]$ ^[25] which gave 99% conversion after 2h of reaction time.

Table 7. Conversion of thymol (for 1.5 g, 0.010 mol), TOF and product selectivity using complex **3** as a catalyst precursor in 2 h of reaction time under different reaction conditions

Entry No.	Catalyst [g (mmol)]	H ₂ O ₂ [g (mmol)]	KBr [g (mmol)]	HClO ₄ [g (mmol)]	Conv [%]	TOF ^a [h ⁻¹]	Selectivity [%] ^b		
							2-Brth	4-Brth	2,4-dBrth
1	0.001 (2.1×10 ⁻³)	1.10 (10)	1.2 (10)	1.4 (10)	98	2289	5	46	49
2	0.015 (3.2×10 ⁻²)	1.10 (10)	1.2 (10)	1.4 (10)	99	154	6	46	48
3	0.002 (4.8×10 ⁻³)	1.10 (10)	1.2 (10)	1.4 (10)	99	1156	7	43	50
4	0.001 (2.1×10 ⁻³)	1.70 (15)	1.2 (10)	1.4 (10)	98	2289	3	91	6
5	0.001 (2.1×10 ⁻³)	2.27 (20)	1.2 (10)	1.4 (10)	99	2313	2	92	6
6	0.001 (2.1×10 ⁻³)	1.10 (10)	1.7 (15)	1.4 (10)	98	2289	6	38	56
7	0.001 (2.1×10 ⁻³)	1.10 (10)	2.3 (20)	1.4 (10)	99	2313	7	30	63
8	0.001 (2.1×10 ⁻³)	1.10 (10)	1.2 (10)	2.1 (15)	99	2313	8	16	76
9	0.001 (2.1×10 ⁻³)	1.10 (10)	1.2 (10)	2.8 (20)	99	2313	7	9	84
10	0.001 (2.1×10 ⁻³)	1.10 (10)	1.2 (10)	1.4 (10)	98	2289	5	46	49
11	-----	1.10 (10)	1.2 (10)	1.4 (10)	32	8	68	24

a) TOF values calculated at 2 h of reaction time.

The other three catalysts, *i.e.* complexes **1**, **2** and **4** were also tested under the above reaction conditions for the maximum conversion of thymol in 2 h of reaction time and the results are summarized in Table 8. The catalytic potential of these complexes compares well with results obtained with other metal complexes, such as: [V^VO(acac)(6,6'-(2-(pyridin-2yl)ethylazanediy)bis(methylene)-bis(2,4-di-tertbutylphenol))],^[5e] Cs(H₂O)[V^VO₂(3,5-bis(2-hydroxyphenyl)-1-phenyl-1,2,4-triazole)]^[5b] and [Mo^{VI}O₂(8-formyl-7-hydroxy-4-methylcoumarin-bhz)(MeOH)]^[25] which gave 99% conversion after 2h of reaction time.

Table 8. Conversion of thymol (1.5 g, 0.010 mol), TOF and selectivity of different products using different catalysts in 2 h of reaction time under optimized reaction conditions.

Entry	Complex (g)	Conv. [%]	TOF [h ⁻¹] ^a	Selectivity [%]		
				2-Brth	4-Brth	2,4-dBrth
1.	1 (0.001)	98	2300	5	46	49
2.	2 (0.001)	90	2112	14	68	18
3.	3 (0.001)	98	2289	9	30	61
4.	4 (0.001)	95	2188	18	40	42

^aTOF values calculated at 2 h of reaction time.

Oxidation of Alkenes

Our previous research has shown that vanadium complexes of hydrazone ligands are good homogeneous catalysts for the oxidation of olefins, hence, we continued our studies with the complexes synthesized here and examined their ability to catalyze the epoxidation of various alkenes, namely styrene, cyclohexene, *cis*-cyclooctene, 1-hexene, 1-octene, cyclohexanone and *trans*-stilbene as model substrates. The oxidation of *cis*-cyclooctene, as a representative substrate of olefins, was carried out in the presence of $[\text{K}(\text{H}_2\text{O})_2][\text{VO}_2(\text{dar-inh})]$ (**1**) as representative homogeneous catalyst to find the optimal conditions for the epoxidation of *cis*-cyclooctene.

To achieve suitable reaction conditions various parameters were screened, taking 5 mmol (0.55 g) of *cis*-cyclooctene and 6 h of reaction time: the amount of catalyst, i.e. complex **1**; amount of oxidant, i.e. aqueous 30% H_2O_2 , amount of NaHCO_3 ; nature of solvent, the solvent volume; and the temperature. Table 9 summarizes all the conditions and conversions obtained and Figure S7 presents conversion-time curves. The optimal reaction conditions for the epoxidation of 5 mmol of *cis*-cyclooctene are (entry 5): catalyst (0.0005 g), 30% H_2O_2 (1.70 g, 15 mmol), NaHCO_3 (2 mmol), MeCN (7 mL) and 80 °C of reaction temperature. Under these conditions, the reaction requires 6 h to give a maximum of 85% conversion with 100% selectivity for cyclooctene oxide. Other solvents were tested under the optimised reaction conditions, and in general gave lower conversions, when compared to MeCN, following the order: EtOH (78%) > MeOH (56%) > CH_3Cl (29%) > CH_2Cl_2 (20%) > n-hexane (12%) > toluene (10%). Low solubility of the complexes in non-polar solvents is possibly the reason for the poor results in this type of solvents. We have also tested K_2CO_3 and NaOH as promoters, instead of NaHCO_3 , but both of them did not perform well (39% conversion using K_2CO_3 and only 2% using NaOH). The blank reaction (entry 12) under the optimized conditions gave only 30% conversion.

Various other alkenes were screened, namely styrene, 1-octene, 1-hexene, *trans*-stilbene, cyclohexene and 2-cyclohexenone in the above reaction conditions after 6 and 24 h of reaction time using all catalysts and the results are summarized in Table 10; conversion profiles for *cis*-cyclooctene as a representative substrate, with all four catalysts are presented in Figure 11.

Table 9. Conversion of *cis*-cyclooctene (0.55 g, 0.005 mol) using $[\text{K}(\text{H}_2\text{O})_2][\text{VO}_2(\text{dar-inh})]$ (**1**) as catalyst precursor under different reaction conditions in the presence of NaHCO_3 in 6 h of reaction time.

Entry No.	Catalyst (g)	H_2O_2 g (mmol)	NaHCO_3 g (mmol)	Temp. [°C]	MeCN [mL]	Conv. [%]	Select. %
1	0.0005(1.06×10^{-3})	2.27 (20)	0.168 (2)	80	7	85	100
2	0.001 (2.13×10^{-3})	2.27 (20)	0.168 (2)	80	7	86	100
3	0.002 (4.26×10^{-3})	2.27 (20)	0.168 (2)	80	7	87	100
4	0.005 (1.06×10^{-3})	1.10 (10)	0.168 (2)	80	7	72	100
5	0.005 (1.06×10^{-3})	1.70 (15)	0.168 (2)	80	7	85	100
6	0.005 (1.06×10^{-3})	1.70 (15)	0.084 (1)	80	7	73	100
7	0.005 (1.06×10^{-3})	1.70 (15)	0.252 (3)	80	7	86	100
8	0.005 (1.06×10^{-3})	1.70 (15)	0.168 (2)	60	7	60	100
9	0.005 (1.06×10^{-3})	1.70 (15)	0.168 (2)	70	7	75	100
10	0.005 (1.06×10^{-3})	1.70 (15)	0.168 (2)	80	5	58	100
11	0.005 (1.06×10^{-3})	1.70 (15)	0.168 (2)	80	9	71	100
13	-----	1.70 (15)	0.168 (2)	80	7	30	100
14	-----	1.70 (15)	-----	80	7	-----	-----
15	0.005 (1.06×10^{-3})	1.70 (15)	-----	80	7	-----	-----

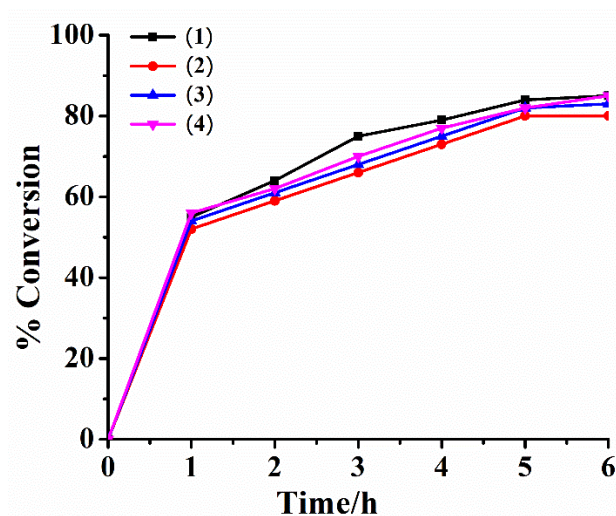
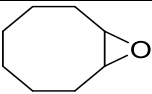
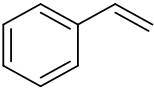
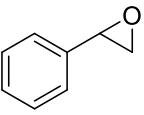
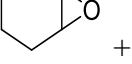
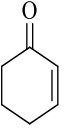
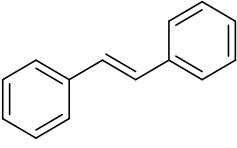
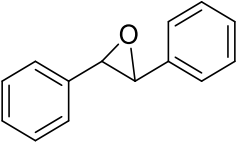
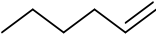
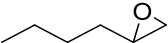
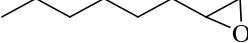


Figure 11 Plots representing conversion of *cis*-cyclooctene in the presence of different vanadium complexes as catalysts.

In general, after 6 h the conversion of aromatic olefins is above 80% and reaches *ca.* 99% in 24 h. Conversion of aliphatic olefins (1-octene and 1-hexene) is lower with all these catalysts and 1-hexene shows better results than 1-octene (65-73% vs. 32-52%) in 6 h; and after 24 h the conversion reaches 97-99%. In general, the epoxide is obtained selectively, as no additional signals are observed in the GC for any other product, except in the oxidation of styrene and cyclohexene that form two reaction products, with the major product being the epoxide (see Table 10). Blank reactions (*i.e.* in the presence of H₂O₂ and NaHCO₃ but without catalyst) with all alkenes provided only 10-32% conversion. Using NaHCO₃ as promoter along with H₂O₂ not only enhanced the catalytic efficiency but the catalyst also became selective for the epoxidation product. It has been observed earlier that NaHCO₃ in the presence of H₂O₂ instantly produces HCO₄⁻ (peroxymonocarbonate) which is the key compound responsible for the fast formation of an oxidoperoxidovanadium(V) intermediate.^[25] Since the peroxido species is actually responsible for the oxidation of the substrates, the role of the promoter is very important. Thus, these studies indicate that the complexes have very good catalytic potential and that the promoter NaHCO₃ plays a very important role in enhancing the catalytic activity of these complexes.

Table 10. Oxidation of olefins (5 mmol) by different vanadium catalyst (0.0005 g) and 30% aqueous H₂O₂ (15 mmol) as a terminal oxidant and NaHCO₃ (2 mmol) as promoter under the optimized reaction conditions (see text).

Entry	Substrate	Catalyst	Product(s)	Conv. [6h/24h] %	TOF ^[a]	Selectivity [6h/24h] %
1.		1		85/99	668	100/100
		2		80/99	628	100/100
		3		83/99	652	100/100
		4		85/99	668	100/100
		Blank		30		100
2.		1		91/99	715	100/76 ^[b]
		2		80/99	628	100/78 ^[b]
		3		93/99	730	100/92 ^[b]
		4		92/99	723	100/95 ^[b]

		Blank		32		100
3.		1		90/99	707	100/81 ^[c]
		2		85/98	668	100/80 ^[c]
		3		94/99	738	100/89 ^[c]
		4		91/99	715	100/85 ^[c]
		Blank		28		100
4.		1		95/99	746	100/100
		2		94/99	738	100/100
		3		97/99	762	100/100
		4		96/99	754	100/100
		Blank		30		100
5.		1		86/98	675	100/100
		2		80/98	628	100/100
		3		82/97	644	100/100
		4		83/98	652	100/100
		Blank		32		100
6.		1		73/99	573	100/100
		2		65/99	510	100/100
		3		66/99	518	100/100
		4		66/99	518	100/100
		Blank		18		100
7.		1		52/97	408	100/100
		2		44/97	345	100/100
		3		32/98	251	100/100
		4		42/98	330	100/100
		Blank		10		100

[a] Calcd at 6 h as $[\text{h}^{-1}]$.

[b] The selectivity of epoxide after 24 h. Rest is phenyl acetaldehyde formed.

[c] The selectivity of epoxide after 24 h. Rest is 2-cyclohexenol.

The catalytic potential of the vanadium complexes studied here, particularly for the epoxidation of *cis*-cyclooctene using H₂O₂ in the presence of NaHCO₃ (80-85% conversion in 6h of reaction time) compares well with the catalytic potential of other vanadium complexes: [V^VO₂{(E)-(E)-2-(2-(phenyl(pyridin-2-yl)methylene)hydrazinyl)benzo[d]thiazol}] (96% conversion in 5h of reaction time),^[7f] [V^VO₂{(E)-2-(2-(1-(pyridin-2-yl)ethylidene)hydrazinyl)benzo[d]thiazole}] (97%, 5h),^[7g] [V^VO₂(L)][H₂L= isonicotinic acid(2-hydroxy-benzylidene)-hydrazide] (80%, 5h),^[26] PS-[V^{IV}O(2-(2-aminoethoxy)ethanol)] [PS = chloromethylated polystyrene] (83%, 6h),^[27] [V^{IV}O(2-{(E)-[2-chloroethyl]imino}methyl)-2-naphthol)] (80%, 2h)^[7h], [VO(Me₂NCH₂CH₂N(CH₂-2-O-3,5-C₆H₂(^tBu)₂)] (98%, 6h),^[7i] [V^{IV}O(E)-N'-(phenyl(pyridin-2-yl)methylene)isonicotinhydrazide]Cl₂ (83%, 5h),^[28] 2[V^{IV}OL(H₂O)]·CH₃OH[HL=6,6'-((1E,1'E)-((2-hydroxypropane-1,3-diy)bis(azanylylidene))bis(methanylylidene))bis(2-methoxypheno)] (90%, 4h)^[29] and [V^{IV}O(N-(5-bromosalicylidene)-4,5-dinitro-1,2-phenylenediamine)] (64% 6 h).^[30]

Overall our results also compare well with the ones obtained with a few Mo-catalysts which have shown the following values: [MoO₂Cl₂(N,N-dimethylbenzamide)₂] (99/100% conversion at 6h/24h of reaction time),^[31] [MoO₂(1,4-bis(2-hydroxy-benzyl)-(S,S)-2,2'-bipyrrolidine)] (95%, 1h),^[32] [MoO₂Cl₂(pbim)] (82/98%, 6h/24 h),^[33] [Mo₂O₆((S)-4-(1-Phenylpropyl)-1,2,4-triazole)₂] (98/100% ,6h/24h),^[34] [Mo₂O₆(4,4'-di-*tert*-butyl-2,2'-bipyridine)₂] (93/100%, 6h/24h),^[35] (Htrz)₂[Mo₃O₆(O₂)₄(trz)₂]·H₂O (trz = 1,2,4-triazole) (92/99%, 6h/24h),^[36] [{Mo^{VI}O₂(H₂O)]₃ptk(inh)₃ (99/100% 2h/24h),^[37] and [Mo₂O₆(HpypzA)]_n (57/82 %, 6/24 h).^[38]

Reactivity of Vanadium(V) Complexes with H₂O₂

It has been observed that the performance of aqueous H₂O₂ as terminal oxidant in the catalytic epoxidation of olefins is moderate and various oxidation products form.^[39] Performing these reactions in the presence of NaHCO₃, not only improves the performance of the catalysts but the reaction also becomes selective towards the epoxide product.^[4] To clarify this and obtain information on the intermediate species formed during the catalytic reaction, the reactivity of [K(H₂O)₂][VO₂(dar-bhz)] (**3**) with H₂O₂ in the absence and presence of NaHCO₃ was evaluated. Thus, the dropwise addition of H₂O₂ (2.5 M) to a solution of **3** (6.1 × 10⁻⁵ M) in MeOH resulted in a decrease in the intensity and a red shift of the 378 nm band to 385 nm, along with the development of an isosbestic point at 352 nm (Figure 12). Simultaneously, the intense 280 nm band changes to

a shoulder along with a slight increase in intensity. A similar behaviour was observed for complexes **2** and **4** (Figures S8 and S9) and clear isosbestic points were noted for each complex upon reaction with H_2O_2 . In the case of complex **1** (Figure S10), the isosbestic points are not as clear but the changes are stronger. The development of an isosbestic point suggests the formation of a new species, possibly the oxidoperoxidovanadium(V) one, upon reaction of complexes with H_2O_2 .

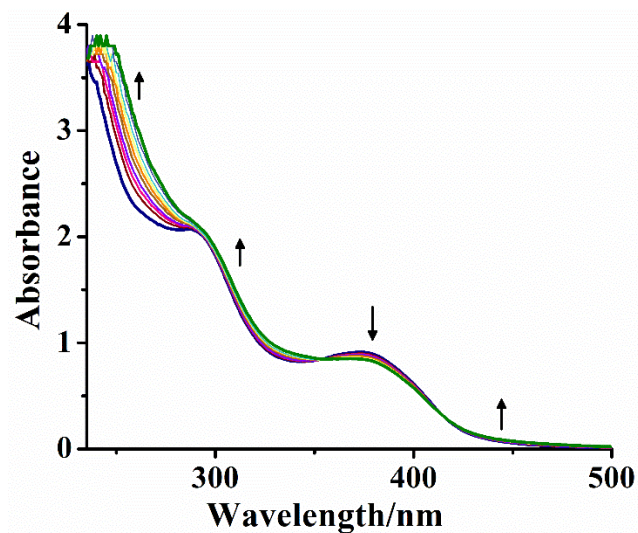


Figure 12. Spectral changes observed during the reactivity of $[\text{K}(\text{H}_2\text{O})_2][\text{VO}_2(\text{dar-bhz})]$ (**3**) with H_2O_2 . The spectra were recorded upon stepwise addition of 2.5 M H_2O_2 solution to 15 mL of 6.1×10^{-5} M solution of **3** in MeOH. Inset shows the expanded view of the 300-500 nm region.

We have also checked the reactivity of two $[\text{V}^{\text{VO}}(\text{OMe})]^{2+}$ type complexes, **7** and **8**, (Figure S11) with H_2O_2 . Thus, the progressive addition of H_2O_2 to a solution of **7** in MeOH (10 mL) resulted in a strong decrease in intensity of the LMCT band at 380 nm (Figure 13) along with the simultaneous formation of an isosbestic point at 348 nm. Two new bands of medium intensity also start developing at 332 and 311 nm. The band at 271 nm only gains intensity while the 210 nm band shifts to 224 nm with the intensity gain. Similar trends have also been observed with complex **8** upon its reaction with H_2O_2 . The change in spectral patterns of these complexes are somewhat different from those observed for anionic complexes **1-4**. The reaction of $[\text{V}^{\text{VO}}(\text{OMe})]^{2+}$ type complexes with H_2O_2 may involve the formation of dioxidovanadium(V) species as an intermediate before converting into oxidoperoxidovanadium(V) species.

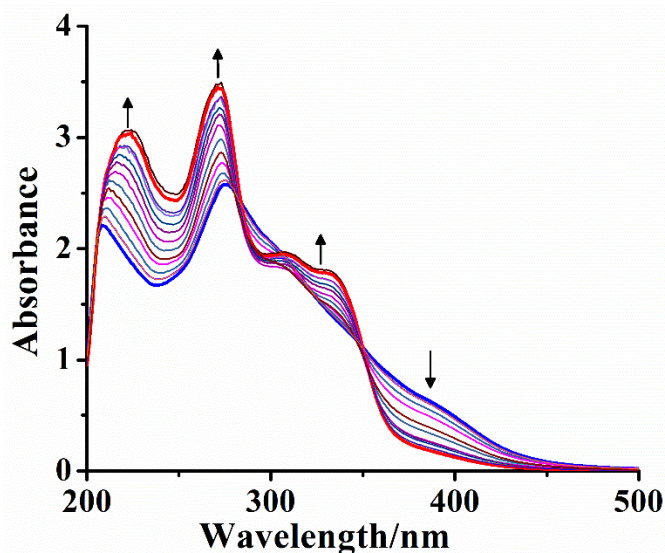
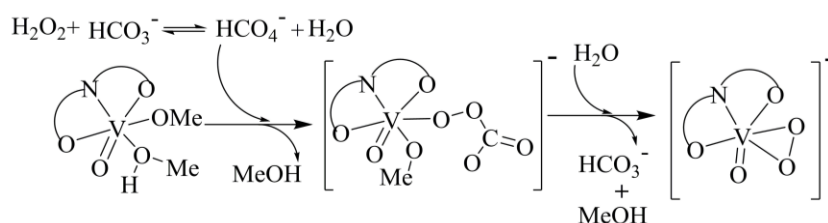


Figure 13. Spectral changes observed during the reactivity of $[\text{VO}(\text{OMe})(\text{MeOH})(\text{dar-bhz})]$ (**7**) with H_2O_2 . (a) The spectra were recorded upon stepwise addition of one drop portions of 1.82×10^{-1} M H_2O_2 solution to 10 mL of 2.26×10^{-5} M solution of **7** in MeOH.

To understand the combined effect of NaHCO_3 and H_2O_2 during the catalytic reaction, a mixture of NaHCO_3 and H_2O_2 dissolved in MeOH was added dropwise to $[\text{K}(\text{H}_2\text{O})_2][\text{VO}_2(\text{dar-bhz})]$ (**3**) and $[\text{VO}(\text{OMe})(\text{MeOH})(\text{dar-bhz})]$ (**7**) solutions. Surprisingly, after adding only a few drops of the mixture of NaHCO_3 and H_2O_2 , very similar and immediate spectral changes could be obtained (Figures 14 and S12) as the ones observed by adding higher amounts of H_2O_2 alone to the above complexes, hinting the quick formation of a similar oxidoperoxido species (Scheme 4) in solution. It has been reported in the literature that NaHCO_3 reacts with H_2O_2 instantly producing HCO_4^- (peroxymonocarbonate).^[39]



Scheme 4. Proposed mechanism for the formation of oxidoperoxidovanadium(V) complex by reaction of complex with H_2O_2 in the presence of NaHCO_3 .

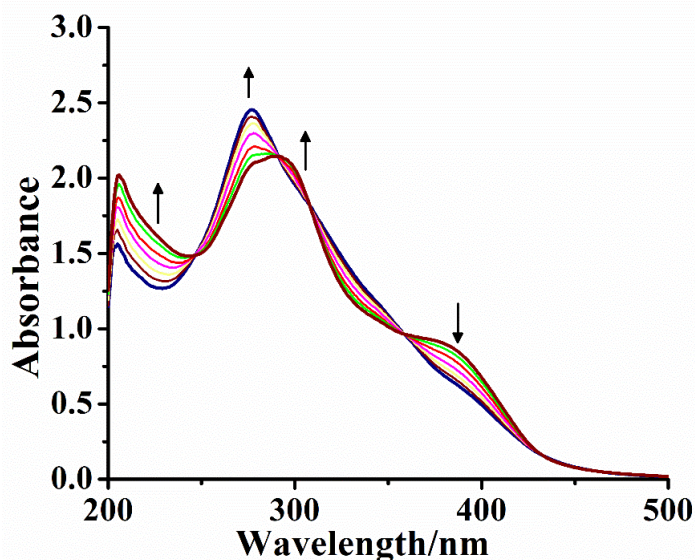


Figure 14. Spectral changes observed during the reactivity of $[\text{VO}(\text{OMe})(\text{MeOH})(\text{dar-bhz})]$ (**7**) with H_2O_2 in the presence of NaHCO_3 . The spectra were recorded upon stepwise addition of one drop portions of a mixture of NaHCO_3 (0.010 g) and 1.52×10^{-1} M H_2O_2 dissolved in 10 mL of MeOH to 20 mL of 2.27×10^{-5} M solution of **7** in MeOH.

The reactivity of the complexes towards H_2O_2 was also evaluated with ^{51}V NMR spectroscopy. Upon addition of H_2O_2 to the complex solutions in MeOH it was interesting to note that while the spectra measured for complexes **7** and **8**, showed the appearance of new species upfield (Figure 15), the other complexes maintained its structure and no new species were formed, except when very high excesses of peroxide were added. In some cases, even after the addition of very high excesses of 30% H_2O_2 solution no new resonances were detected. For these two VOL^+ complexes upon addition of aqueous H_2O_2 to the solutions of the complexes the resonance at *ca.* -540 ppm progressively disappeared and a new resonance appeared at *ca.* -575 ppm, probably corresponding to the oxidoperoxocomplex $\text{V}^{\text{VO}}(\text{O}_2)\text{L}$.^[40] When excess H_2O_2 was added a new peak was observed at *ca.* -655 ppm, which we assign to an inorganic diperoxidovanadate, $[\text{V}^{\text{VO}}(\text{O}_2)_2]^-$.^[41] In general for the VO_2L^- complexes **1-4** no peroxido species could be identified by ^{51}V NMR. The complexes seem very stable as even in the presence of high excess of H_2O_2 no inorganic peroxidovanadates were formed. The exception is complex **1**, which in DMSO shows the presence of another peak upfield. The reason may simply be electronic, due to repulsion between the negatively charged complexes and the peroxide.

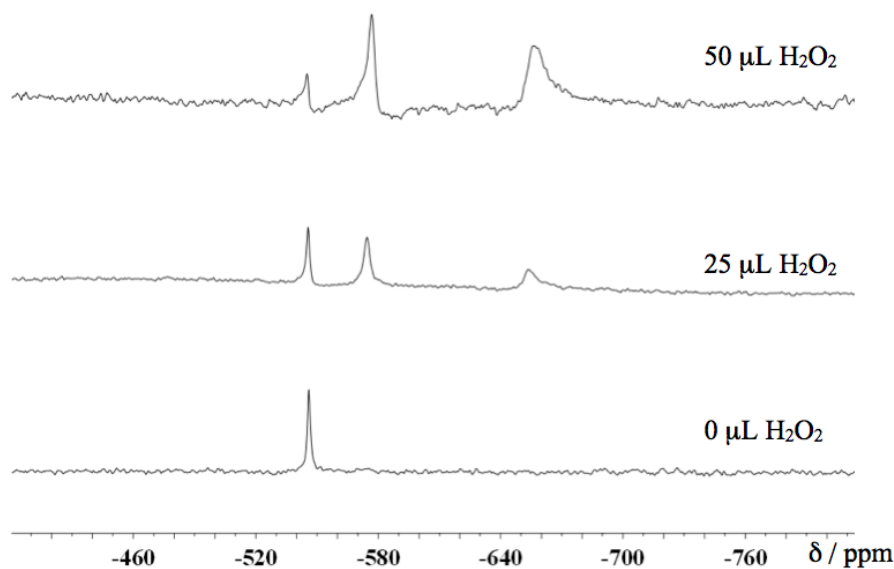


Figure 15 ^{51}V NMR spectra measured for a solution of **8** in MeOH containing 10% MeOD in the absence and presence of H_2O_2 1M.

Conclusions

Dioxidovanadium(V) and oxidomethoxidovanadium(V) complexes with general composition $[\text{K}(\text{H}_2\text{O})_2][\text{V}^{\text{V}}\text{O}_2\text{L}]$ and $[\text{V}^{\text{V}}\text{O}(\text{L})(\text{OMe})(\text{MeOH})]$ where H_2L is a dibasic tridentate ONO ligand derived from 4,6-diacetylresorcinol and various hydrazides have been synthesized and characterized successfully. Single-crystal X-ray diffraction studies confirmed the molecular structures of complexes $[\text{K}(\text{H}_2\text{O})(\text{EtOH})][\text{V}^{\text{V}}\text{O}_2(\text{dar-inh})]$ (**1a**, where one molecule of water is replaced by EtOH), $[\text{V}^{\text{V}}\text{O}(\text{OMe})(\text{MeOH})(\text{dar-nah})]$ (**6**), $[\text{V}^{\text{V}}\text{O}(\text{OMe})(\text{MeOH})(\text{dar-bhz})]$ (**7**) and $[\text{V}^{\text{V}}\text{O}(\text{OMe})(\text{MeOH})(\text{dar-fah})]$ (**8**). The molecular structure of **1a** shows a dimeric structure due to the presence of electrostatic interactions between $\text{V}=\text{O}$ oxygen atoms with K^+ ions and water molecules act as bridges between two K^+ ions. These complexes show excellent catalytic potential towards the oxidative bromination of thymol in the presence of KBr , HClO_4 and H_2O_2 giving 2-bromothymol, 4-bromothymol and 2,4-dibromothymol. They also catalyse the oxidation of olefins in the presence of NaHCO_3 and give the corresponding epoxide selectively. Thus, the synthesized complexes are good structural and functional models of the vanadate-dependent haloperoxidases.

Experimental Section

Materials, Instrumentation and Physical measurements: Chemicals and solvents used in this study were of analytical reagent grade and acquired from standard sources. Precursors $[\text{V}^{\text{IV}}\text{O}(\text{acac})_2]$ ^[42], 4,6-diacetylresorcinol and ligands $\text{H}_2\text{dar-inh}$ (**I**), $\text{H}_2\text{ap-nah}$ (**II**), $\text{H}_2\text{dar-bhz}$ (**III**) and $\text{H}_2\text{dar-fah}$ (**IV**)^[18] were prepared according to methods reported in the literature. Elemental analysis (C, H and N) of ligands and complexes were performed in an Elementar Vario-EI-III instrument. IR Spectra were recorded in KBr on a Nicolet NEXUS Aligent 1100 series FT-IR spectrometer. Electronic spectra of ligands in DMSO and complexes in MeOH were recorded using Shimadzu 2450 UV-Vis spectrophotometer. ^1H and ^{13}C NMR spectra of ligands and complexes were recorded in DMSO- d_6 with JEOL (400 MHz) spectrometer using common parameter settings. The ^{51}V NMR spectra were recorded using a Bruker Advance III 400 MHz spectrometer with the following acquisition parameters: spectral width 3960 ppm, acquisition time 39 ms, line broadening 100 Hz, dwell time 1.200, frequency 105 MHz, free induction decay (FID) resolution 13 Hz, receiver gain 2050, and number of scans > 1500. The ^{51}V NMR spectra were recorded with samples in MeOH and DMSO containing 10 % of deuterated solvent, and the ^{51}V chemical shifts (δ_{V}) are referenced to neat $\text{V}^{\text{V}}\text{OCl}_3$ as internal standard. The chemical shifts of the ^1H and ^{13}C NMR spectra are quoted relative to tetramethyl silane (TMS) as an internal standard. The thermogravimetric analyses of the complexes were acquired under oxygen atmosphere with a TG Stanton Redcroft STA 780 instrument. The catalytic reactions were monitored by a Shimadzu 2010 plus gas chromatograph fitted with an Rtx-1 capillary column (30 m \times 0.25 mm \times 0.25 μm) and a FID detector. The product formation was confirmed in a GC-MS model Perkin-Elmer, Clarus 500 by comparing the fragments of each product with the library available.

Preparation of Complexes

$[\text{K}(\text{H}_2\text{O})_2][\text{VO}_2(\text{dar-inh})]$ (1**):** V_2O_5 (0.18 g, 0.0010 mol) was dissolved in an aqueous solution of KOH (0.11 g, 0.0020 mol in 5-6 mL of H_2O) and stirred for 2 h with occasional heating on a water bath. The resulting clear solution was then filtered. A filtered solution of **I** (0.626 g, 0.0020 mol) dissolved in 30 mL of aqueous KOH (0.22 g, 0.0040 mol) was added to the above solution. The resulting mixture was allowed to react for 2 h with stirring at room temperature and then the pH was adjusted to ca. 7.5 with 2 M HCl. The yellowish colored solid started to form within 30 min but the stirring was continued for 3 h. The solid was filtered, washed with cold water (2 \times 5 mL) and dried in a desiccator over silica gel. Yield: 0.35 g (74 %). $\text{C}_{16}\text{H}_{17}\text{N}_3\text{O}_8\text{VK}$ (469.33 g mol⁻¹)

¹): calcd. C, 40.94; H, 3.65; N, 8.95. found C, 40.43; H, 3.55; N, 8.89%. ESI-MS (MeOH) m/z [Found (Calcd)]: 410.06 (410.27) (80%) $[\text{VO}(\text{MeOH})\text{L}]^+$; 394.32 (394.02) (100%) $[\text{VO}_2\text{L}]^-$. Crystals of **1** suitable for X-ray diffraction studies were grown from 95% ethanolic solution by slow evaporation at room temperature. Crystal of complex **1** is formulated as $[\text{K}(\text{H}_2\text{O})(\text{EtOH})][\text{VO}_2(\text{dar-inh})]$ (**1a**).

$[\text{K}(\text{H}_2\text{O})_2][\text{VO}_2(\text{dar-nah})]$ (2): Yellow complex **2** was prepared by the method described for complex **1** using ligand **II**. Yield: 0.40 g (85 %). $\text{C}_{16}\text{H}_{17}\text{N}_3\text{O}_8\text{VK}$ (469.33 g mol⁻¹): calcd. C, 40.94; H, 3.65; N, 8.95. found C, 40.58; H, 3.43; N, 8.77%. ESI-MS (MeOH) m/z [Found (Calcd)]: 410.24 (410.27) (30%) $[\text{VO}(\text{MeOH})\text{L}]^+$; 394.30 (394.02) (100%) $[\text{VO}_2\text{L}]^-$.

$[\text{K}(\text{H}_2\text{O})_2][\text{VO}_2(\text{dar-bhz})]$ (3): Yellow complex **3** was prepared by the method described for complex **1** using ligand **III**. Yield: 0.33 g (70 %). $\text{C}_{17}\text{H}_{18}\text{N}_2\text{O}_8\text{VK}$ (468.38 g mol⁻¹): calcd. C, 43.59; H, 3.87; N, 5.98. found C, 43.08; H, 3.65; N, 5.90%. ESI-MS (MeOH) m/z [Found (Calcd)]: 335.36 (335.02) (50%) $[\text{VOL}]^+$; 393.38 (393.03) (100%) $[\text{VO}_2\text{L}]^-$.

$[\text{K}(\text{H}_2\text{O})_2][\text{VO}_2(\text{dar-fah})]$ (4): Yellow complex **4** was prepared by the method described for complex **1** using ligand **IV** as ligand. Yield: 0.35 g (76 %). $\text{C}_{15}\text{H}_{16}\text{N}_2\text{O}_9\text{VK}$ (458.34 g mol⁻¹): calcd. C, 39.31; H, 3.52; N, 6.11. found C, 40.33; H, 3.54; N, 5.76%. ESI-MS (MeOH) m/z [Found (Calcd)]: 399.15 (399.04) (45%) $[\text{VO}(\text{MeOH})\text{L}]^+$; 383.33 (383.01) (100%) $[\text{VO}_2\text{L}]^-$.

$[\text{V}^{\text{VO}}(\text{OMe})(\text{MeOH})(\text{dar-inh})]$ (5): Complex **1** (0.469 g, 0.0010 mmol) was dissolved in methanol (30 mL) and refluxed on a water bath for 4 h. The obtained clear solution was allowed to stand in the open flask for slow evaporation. The yellow solid slowly precipitated out within a week. This was filtered, washed with methanol followed by petroleum ether (b.p. 60 °C) and dried in a desiccator over silica gel. Yield: 0.32 g (68 %). $\text{C}_{18}\text{H}_{20}\text{N}_3\text{O}_7\text{V}$ (441.31 g mol⁻¹): calcd. C, 48.99; H, 4.57; N, 9.52. found C, 48.44; H, 4.50; N, 9.23%. ESI-MS (MeOH) m/z [Found (Calcd)]: 410.21 (410.06) (100%) $[\text{VO}(\text{MeOH})\text{L}]^+$; 394.48 (394.02) (100%) $[\text{VO}_2\text{L}]^-$.

$[\text{V}^{\text{VO}}(\text{OMe})(\text{MeOH})(\text{dar-nah})]$ (6): Yellow Complex **6** was prepared from **2** by the method described for complex **5**. Yield: 0.34 g (77 %). $\text{C}_{18}\text{H}_{20}\text{N}_3\text{O}_7\text{V}$ (441.31 g mol⁻¹): calcd. C, 48.99; H, 4.57; N 9.52. found C, 48.40; H, 4.50; N, 9.20%. ESI-MS (MeOH) m/z [Found (Calcd)]: 410.25 (410.06) (35%) $[\text{VO}(\text{MeOH})\text{L}]^+$; 394.40 (394.02) (100%) $[\text{VO}_2\text{L}]^-$. Crystals of **1** suitable for X-ray diffraction studies were grown by slow evaporation of a methanolic solution of **2** at room temperature within a week.

[V^VO(OMe)(MeOH)(dar-bhz) (7): Ligand **III** (0.31 g, 0.0010 mol) was dissolved in methanol (15 mL) and filtered. A solution of [V^VO(acac)₂] (0.26 g, 0.0010 mol) in methanol (15 mL) was added to the above solution with stirring. The reaction mixture was refluxed on a water bath for *ca.* 6 h. The obtained black colored solution was reduced to 10 mL and kept in the refrigerator (*ca.* 5 °C) from which a black solid slowly precipitated out. The solid was filtered, washed with methanol followed by petroleum ether (b.p. 60 °C) and dried in a desiccator over silica gel. Yield: 0.33 g (75 %). Crystals of **7** suitable for X-ray diffraction studies were obtained from the filtrate by slow evaporation at room temperature. C₁₉H₂₁N₂O₇V (440.33 g mol⁻¹): calcd. C, 51.83; H, 4.81; N, 6.36. found C, 51.39; H, 4.50; N, 6.71%. ESI-MS (MeOH) *m/z* [Found (Calcd)]: 409.14 (409.06) (100%) [VO(MeOH)L]⁺; 393.30 (393.03) (60%) [VO₂L]⁻.

[V^VO(OMe)(MeOH)(dar-fah) (8): Black complex **8** was prepared by the method described for complex **7** using ligand **IV**. Yield: 0.32 g (72 %). Crystals of **8** suitable for X-ray diffraction studies were obtained from the filtrate by slow evaporation at room temperature. C₁₇H₁₉N₂O₈V (430.29 g mol⁻¹): calcd. C, 51.83; H, 4.81; N, 6.36. found C, 51.48; H, 4.74; N, 6.07%. ESI-MS (MeOH) *m/z* [Found (Calcd)]: 399.12 (399.04) (50%) [VO(MeOH)L]⁺; 383.22 (383.01) (35%) [VO₂L]⁻.

X-Ray crystal structure determination

Three-dimensional X-ray data were collected on a Bruker Kappa Apex CCD diffractometer at room temperature for compounds **1a**, **6** and **8** and at low temperature for compound **7**, by the ϕ - ω scan method. Reflections were measured from a hemisphere of data collected from frames, each of them covering 0.3° in ω . A total of 12795 reflections were measured for **1a**, 33908 for **6**, 10062 for **7** and 15211 for **8**, and corrected for Lorentz and polarization effects and for absorption by multi-scan methods based on symmetry-equivalent and repeated reflections. Of the total, 2888 independent reflections for **1a**, 3360 for **6**, 2554 for **7** and 3926 for **8**, exceeded the significance level ($|F|/\sigma|F|$) > 4.0. After data collection, in each case a multi-scan absorption correction (SADABS)^[43] was applied, and the structures were solved by direct methods and refined by full matrix least-squares on F^2 data using SHELX suite of programs.^[44] Hydrogen atoms were included in calculated positions and refined in the riding mode for all structures, except for O(7) in **1a**, which was located in difference Fourier map and fixed to the oxygen atom, for O(1M) and O(4) in **6**, for O(1s) and O(4) in **7** and for O(1M), C(2), O(5), C(13) and C(13) in **8**, which were located in difference Fourier maps and left to refine freely. Refinements were done with allowance for

thermal anisotropy of all non-hydrogen atoms. A final difference Fourier map showed no residual density outside: 1.164 and -1.423 e.Å⁻³ for **1a**, 0.434 and -0.498 e.Å⁻³ for **6**, 0.513 and -0.574 e.Å⁻³ for **7** and 0.480 and -0.497 e.Å⁻³ for **8**. A weighting scheme $w = 1/[\sigma^2(F_o^2) + (0.184600 P)^2 + 0.00000 P]$ for **1a**, $1/[\sigma^2(F_o^2) + (0.068400 P)^2 + 1.694500 P]$ for **6**, $1/[\sigma^2(F_o^2) + (0.091700 P)^2 + 0.00000 P]$ for **7** and $1/[\sigma^2(F_o^2) + (0.081800 P)^2 + 0.111700 P]$ for **8**, where $P = (|F_o|^2 + 2|F_c|^2)/3$, were used in the latter stages of refinement. Further details of the crystal structures determination are given in Table 11. CCDC 1858915-1858918 contain the supplementary crystallographic data for the structures reported in this paper. These data can be obtained free of charge via <http://www.ccdc.cam.ac.uk/conts/retrieving.html>, or from the Cambridge Crystallographic Data Centre, 12 Union Road, Cambridge CB2 1EZ, UK; fax: (+44) 1223 336 033; or e-mail: deposit@ccdc.cam.ac.uk. Supplementary data associated with this article can be found, in the online version, at doi: \$\$\$\$\$\$.

Table 11. Crystal Data and Structure Refinement for the compounds **1a**, **6**, **7** and **8**.

	1a	6	7	8
	(CCDC 1858915)	(CCDC 1858916)	(CCDC 1858917)	(CCDC 1858918)
Formula	C ₁₈ H ₂₁ KN ₃ O ₈ V	C ₁₈ H ₂₀ N ₃ O ₇ V	C ₁₉ H ₂₁ N ₂ O ₇ V	C ₁₇ H ₁₉ N ₂ O ₈ V
Formula weight	497.42	441.31	440.32	430.28
T, K	293(2)	293(2)	100(2)	296(2)
Wavelength, Å	0.71073	0.71073	0.71073	0.71073
Crystal system	Triclinic	Orthorhombic	Triclinic	Triclinic
Space group	P $\bar{1}$	Pbca	P $\bar{1}$	P $\bar{1}$
<i>a</i> /Å	7.3180(13)	7.4643(4)	7.9783(10)	7.9398(12)
<i>b</i> /Å	11.8167(17)	13.5914(6)	9.1722(10)	9.0589(14)
<i>c</i> /Å	13.037(2)	38.0274(17)	13.8205(17)	13.768(2)
α /°	106.127(9)	90	99.863(9)	77.711(7)
β /°	104.472(9)	90	92.801(9)	85.623(7)
γ /°	97.322(9)	90	104.733(9)	79.714(7)
<i>V</i> /Å ³	1024.9(3)	3857.9(3)	959.1(2)	951.3(2)
<i>Z</i>	2	8	2	2
<i>F</i> ₀₀₀	512	1824	456	444
<i>D</i> _{cal} /g cm ⁻³	1.612	1.520	1.525	1.502
μ /mm ⁻¹	0.739	0.561	0.563	0.569
θ (°)	1.70 to 28.42	3.00 to 28.31	1.50 to 26.49	1.51 to 28.30

R_{int}	0.0726	0.0539	0.0569	0.0281
Crystal size/ mm ³	0.33×0.21×0.09	0.30×0.20×0.10	0.38×0.07×0.07	0.34×0.28×0.11
Goodness-of-fit on F^2	0.985	1.076	1.049	1.130
$R_1[I > 2\sigma(I)]^a$	0.0859	0.0458	0.0644	0.0362
wR_2 (all data) ^b	0.2782	0.1402	0.1763	0.1334
Largest differences peak and hole (e ^Å ⁻³)	1.164 and -1.423	0.434 and -	0.513 and -	0.480 and -0.497

$$^a R_1 = \frac{\sum ||F_o| - |F_c||}{\sum |F_o|} \quad ^b wR_2 = \left\{ \frac{\sum [w(|F_o|^2 - |F_c|^2)]^2}{\sum [w(F_o^2)]} \right\}^{1/2}$$

⁵¹V NMR Studies

Solutions for ⁵¹V NMR were prepared in MeOH and/or DMSO, in order to obtain *ca.* 2-3 mM solutions. For **7** in DMSO there were still traces of solid, even when diluted to 1.8 mM. In MeOH only complexes **1** and **3** dissolved but the spectra for the others were measured with solutions having traces of solid. All samples contained 10% of the corresponding deuterated solvent. The aqueous H₂O₂ (30% w/v) was diluted 1:10 in D₂O and added to the samples. For **5**, since no new peaks appeared after addition of this peroxide solution, a concentrated solution was added.

Bromination of Thymol

In order to obtain the best reaction conditions for the bromination of thymol several parameters were changed, such as the amount of catalyst, KBr, H₂O₂ and HClO₄ using **3** as a representative catalyst. Thus, for 0.010 moles (1.5 g) of thymol, three different amounts of catalyst (0.001, 0.015, and 0.002 g), KBr (0.010, 0.015, and 0.020 moles), H₂O₂ (0.010, 0.015, and 0.020 moles) and HClO₄ (0.010, 0.015, and 0.030 moles) were taken in 20 mL H₂O, and the reactions were carried out at room temperature for 2 h. When addition of HClO₄ was more than 0.010 moles, it was added in two equal portions for 0.015 moles and three equal portions for 0.030 moles; first addition at $t = 0$ and the others at every half an hour interval to avoid decomposition of the catalyst.

Oxidation of Alkenes

In order to achieve suitable reaction conditions for the epoxidation of *cis*-cyclooctene, various reaction conditions were studied, *i.e.* 5 mmol (0.55 g) of *cis*-cyclooctene, three different amounts of catalyst, *i.e.* complex **1** (0.0005, 0.001 and 0.0020 g) and aqueous 30% H₂O₂ (10, 15 and 20

mmol), three different volumes of solvent (MeCN: 5, 7 and 9 mL) and the reaction was carried out in the presence of NaHCO₃ (1, 2 and 3 mmol) at three different temperatures (60, 70 and 80 °C) for 6h of reaction time with stirring on an oil bath.

Initially to optimize the amount of catalyst, 5 mmol (0.55 g) of *cis*-cyclooctene and three different amounts of representative catalyst (**1**), 0.0005, 0.001 and 0.002 g, were taken while keeping all other reaction parameters constant as 30 % H₂O₂ (1.70 g, 15 mmol), NaHCO₃ (0.168 g, 2 mmol) and MeCN (7 mL) at 80 °C for 6 h of reaction time. To see the effect of the amount of oxidant on the oxidation of *cis*-cyclooctene, three different amounts of oxidant i.e. (1.130 g, 10 mmol), (1.69 g, 15 mmol), (2.270 g, 20 mmol) of 30% H₂O₂ were taken keeping all other reaction parameters constant as catalyst (0.0005 g), NaHCO₃ (0.168 g, 2 mmol) and MeCN (7 mL) at 80 °C. Three different amounts of NaHCO₃ i.e. 1 mmol (0.084 g), 2 mmol (0.126 g) and 3 mmol (0.168 g) were considered for the other fixed reaction parameters i.e. catalyst (0.0005 g), 30 % H₂O₂ (1.70 g, 15 mmol) and MeCN (7 mL) and reaction was carried out at of 80 °C for 6h to obtained suitable amount of promoter. The effect of the temperature on the oxidation of *cis*-cyclooctene was studied for three different temperatures (60, 70 and 80 °C) while keeping other reaction parameters fixed as optimized above. The amount of solvent was screened with three different volumes of MeCN (5, 7 and 9 mL).

Acknowledgments

M. R. M. thanks the Science and Engineering Research Board (SERB), Government of India, New Delhi, for financial support of the work (grant number EMR/2014/000529). N. J. is thankful to the Indian Institute of Technology (IIT) Roorkee, India, for the Institute fellowship. I. C. thanks Fundação para a Ciência e Tecnologia (project UID/QUI/00100/2013) and Investigador FCT programme. The Portuguese NMR and Mass Spectrometry IST–UL Centres are acknowledged for the access to the equipment.

References

- [1] D. Rehder, *Bioinorganic Vanadium Chemistry*, John Wiley & Sons, New York, 2008.
- [2] a) J. O. Nriagu (Ed.), *Vanadium in the Environment*, John Wiley, New York, 1998; b) A. Butler, A. H. Baldwin, “Vanadium bromoperoxidase and functional mimics” in *Metal sites in proteins and models*, Volume 89 of the series “Structure and Bonding” pp 109-132; c) A.

- Butler and C. J. Carrano, *Coord. Chem. Rev.* **1991**, *109*, 61–105; d) D. Rehder, *Coord. Chem. Rev.* **1999**, *182*, 297–322; e) H. Michibata, N. Yamaguchi, T. Uyama, T. Ueki, *Coord. Chem. Rev.* **2003**, *237*, 41–51; f) M. R. Maurya, *Coord. Chem. Rev.* **2003**, *237*, 163–181; g) D. Rehder, G. Santoni, G.M. Licini, C. Schulzke, B. Meier, *Coord. Chem. Rev.* **2003**, *237*, 53–63.
- [3] a) M. R. Maurya, S. Agarwal, C. Bader, M. Ebel and D Rehder, *Dalton Trans.* **2005**, 537–544; b) M. R. Maurya, S. Agarwal, C. Bader and D. Rehder, *Eur. J. Inorg. Chem.* **2005**, 147–157; c) M. R. Maurya, A. Kumar, M. Ebel, D. Rehder, *Inorg. Chem.* **2006**, *45*, 5924–5937; d) M. R. Maurya, B. Sarkar, F. Avecilla, and I. Correia, *Eur. J. Inorg. Chem.* **2016**, 4028–4044; e) M. R. Maurya, C. Haldar, A. Kumar, M.L. Kuznetsov, F. Avecillac, J. C. Pessoa, *DaltonTrans.* **2013**, *42*, 11941-11962.
- [4] M. Sutradhar, L.M.D.R.S. Martins, M.F.C.G. da Silva, A.J.L. Pombeiro, *Coord. Chem. Rev.* **2015**, *301–302*, 200–239.
- [5] a) S. Barroso, P. Adão, F. Madeira, M. T. Duarte, J. Costa Pessoa and A. M. Martins, *Inorg. Chem.* **2010**, *49*, 7452–7463; b) M. R. Maurya, B. Sarkar, F. Avecilla, S. Tariq, A. Azam, and I. Correia, *Eur. J. Inorg. Chem.* **2016**, 1430–1441; c) S. P. Dash, A. K. Panda, S. Dhaka, S. Pasayat, A. Biswas, M. R. Maurya, P. K. Majhi, A. Crochetf and R. Dinda, *Dalton Trans.* **2016**, *45*, 18292-18307; d) V. Conte, B. Floris, *Inorg. Chim. Acta* **2010**, *363*, 1935–1946; e) M. R. Maurya, B. Uprety, F. Avecilla, P. Adão, and J. C. Pessoa, *Dalton Trans.* **2015**, *44*, 17736-17755; f) P. Adak, B. Ghosh, B. Pakhira, R. Sekiya, R. Kuroda, S.K. Chattopadhyay, *Polyhedron* **2017**, *127*, 135–143.
- [6] a) M.F. Litvić, M. Litvić, V.Vinković, *Tetrahedron* **2008**, *64*, 10912–10918; b) J. Su, C. Zhang, D. Lin, Y. Duan, X. Fu and R. Mu, *Synth. Commun.* **2010**, *40*, 595–600; c) M. R. Maurya, A. Arya, A. Kumar, M.L. Kuznetsov, F. Avecilla and J. Costa Pessoa, *Inorg. Chem.* **2010**, *49*, 6586–6600; d) D. Zhang, K. Jamieson, L. Guy, G. Gao, J.P. Dutastab and A. Martinez, *Chem. Sci.*, **2017**, *8*, 789-794; e) M. S. Maru, S. Barroso, P. Adao, L.G. Alves, A. M. Martins, *J. Organomet. Chem.* **2018**, *870*, 136-144; f) G. Romanowski, J. Kira, *Polyhedron* **2016**, *117*, 352–358.

- [7] (a) B. N. Wigington, M. L. Drummond, T. R. Cundari, D. L. Thorn, S. K. Hanson and S. L. Scott, *Chem. Eur. J.* **2012**, *18*, 14981–14988; b) S. Pasayat, M. Bohme, S. Dhaka, S. P. Dash, S. Majumder, M. R. Maurya, W. Plass, W. Kaminsky and R. Dinda, *Eur. J. Inorg. Chem.* **2016**, 1604–1618; d) Y. Zhang, T. Yang, B.Y. Zheng, M. Y. Liu, N. Xing, *Polyhedron* **2017**, *121*, 123–129; e) G. Romanowski, *J. Mol. Catal. A: Chem.* **2013**, *368–369*, 137–144; f) M. Ghorbanloo, S. Jafari, R. Bikas, M. S. Krawczyk, T. Lis, *Inorg. Chim. Acta* **2017**, *455*, 15–24; g) M. Ghorbanloo, R. Bikas, S. Jafaria, M. S. Krawczyk and T. Lis, *J. Coord. Chem.* **2018**; h) V. Tahmasebi, G. Grivani, G. Bruno, *J. of Mol. Struct.* **2016**, *1123*, 367–374; i) F. Madeira, S. Barroso, S. Namorado, P. M. Reis, B. Royo, A. M. Martins, *Inorg. Chim. Acta* **2012**, *383*, 152–156.
- [8] a) M. R. Maurya, C. Haldar, A. A. Khan, A. Azam, A. Salahuddin, A. Kumar and J. Costa Pessoa, *Eur. J. Inorg. Chem.* **2012**, 2560–2577; b) S. D. Kurbah, M. Asthana, I. Syiemlieh, R. A. Lal, *Appl. Organomet. Chem.* **2018**; *32*, 4299; c) B. Chen, X. Huang, B. Wang, Z. Lin, J. Hu, Y. Chi, C. Hu, *Chem. Eur. J.* **2013**, *19*, 4408–4413; d) G. Zhang, B.L. Scott, R. Wu, L.A. P. Silks, S.K. Hanson, *Inorg. Chem.* **2012**, *51*, 7354; e) S. K. Hanson, R. Wu, L. A. P. Silks, *Org. Lett.* **2011**, *13*, 1908–1911.
- [9] (a) M. Sutradhar, M.V. Kirillova, M. F. C. G. da Silva, L. M. D. R. S. Martins, and A. J. L. Pombeiro, *Inorg. Chem.* **2012**, *51*, 11229–11231; b) M. Sutradhar, N. V. Shvydkiy, M. F. C. G. da Silva, M. V. Kirillova, Y. N. Kozlov, A. J. L. Pombeiro and G. B. Shul’pin, *Dalton Trans.* **2013**, *42*, 11791–11803; c) I. Gryca, K. Czerwińska, B. Machura, A. Chrobok, L. S. Shul’pina, M. L. Kuznetsov, D. S. Nesterov, Y. N. Kozlov, A. J. L. Pombeiro, I. A. Varyan, and G. B. Shul’pin, *Inorg. Chem.* **2018**, *57*, 1824–1839; d) D. Dragancea, N. Talmaci, S. Shova, G. Novitchi, D. Darvasiová, P. Rapta, M. Breza, M. Galanski, J. Kožíšek, N. M. R. Martins, L. M. D. R. S. Martins, A. J. L. Pombeiro, and V. B. Arion, *Inorg. Chem.* **2016**, *55*, 9187–9203; e) T. F. S. Silva, K. V. Luzyanin, M. V. Kirillova, M. F. Guedes da Silva, L. M. D. R. S. Martins, A. J. L. Pombeiro, *Adv. Synth. Catal.* **2010**, *352*, 171–187; f) T. F. S. Silva, T. C. O. MacLeod, L. M. D. R. S. Martins, M. F. C. Guedes da Silva, M. A. Schiavon, A. J. L. Pombeiro, *J. Mol. Catal. A: Chem.* **2013**, *367*, 52–60.
- [10] a) M. R. Maurya, U. Kumar, I. Correia, P. Adão, and J. Costa Pessoa, *Eur. J. Inorg. Chem.* **2008**, 577–587; b) M. R. Maurya, A. Arya, U. Kumar, A. Kumar, F. Avecilla and J. Costa

- Pessoa, *Dalton Trans.* **2009**, 9555–9566; c) M. R. Maurya and N. Kumar, *J. Mol. Catal A: Chem.* **2014**, 383–384, 172–181.
- [11] a) M. R. Maurya, B. Sarkar, F. Avecilla and I. Correia, *Dalton Trans.* **2016**, 45, 17343–17364; b) M. R. Maurya, N. Saini and F. Avecilla, *RSC Adv.* **2016**, 6, 12993–13009.
- [12] K. M. Raj, B. Vivekanand, G.Y. Nagesh, B.H.M. Mruthyunjayaswamy, *J. Mol. Struct.* **2014**, 1059, 280–293.
- [13] M. Shebl, M. A. El-ghamry, S. M. E. Khalil, M. A. A. Kishk, *Spectrochim. Acta, Part A: Molecular and Biomolecular Spectroscopy* **2014**, 126, 232–241.
- [14] C. Demetgül, C., *Carbohydrate Polymers* **2012**, 89, 354–361.
- [15] S. P. Netalkar, A. A. Nevrekar, V. K. Revankar, *Cat. Lett.* **2014**, 144, 1573–1583.
- [16] B. S. Lane, K. Burgess, *Chem. Rev.* **2003**, 103, 2457–2473.
- [17] (a) P. Schwendt, J. Tatiersky, L. Krivosudský, M. Šimuněková, *Coord. Chem. Rev.* **2016**, 318, 135–157; (b) M. Sutradhar, L. M. D. R. S Martins, M. F. C. Guedes da Silva, A. J. L. Pombeiro, *Coord. Chem. Rev.* **2015**, 301–302, 200–239.
- [18] M. R. Maurya, L. Rana and F. Avecilla, *Polyhedron* **2017**, 126, 60–71.
- [19] A. Jain, C. S. Purohit, S. Verma and R. Sankararamkrishnan, *J. Phys. Chem. B* **2007**, **111**, 8680–8683.
- [20] A. D. Keramidas, A. B. Papaioannou, A. Vlahos, T. A. Kabanos, G. Bonas, A. Makriyannis, C. P. Raptopoulou, A. Terzis, *Inorg. Chem.* **1996**, 35, 357–367.
- [21] C. Das, P. Adak, S. Mondal, R. Sekiya, R. Kuroda, S. I. Gorelsky, S. K. Chattopadhyay, *Inorg. Chem.* **2014**, 53, 11426–11437.
- [22] a) M. A. Naziria, E. Sahina, N. Seferoglu and B. Shaabanic, *J. Coord. Chem.* **2018**, 71, 89–103.
- [23] S. Kundu, D. Mondal, K. Bhattacharya, A. Endo, D. Sanna, E. Garribba, and M. Chaudhury, *Inorg. Chem.* **2015**, 54, 6203–6215.
- [24] F. Sabuzi, E. Churakova, P. Galloni, R. Wever, F. Hollmann, B. Floris, V. Conte, *Eur. J. Inorg. Chem.* **2015**, 3519–3525.
- [25] M. R. Maurya, S. Dhaka, F. Avecilla, *Polyhedron* **2015**, 96, 79–87.
- [26] H. H. Monfared, A. Farrokhi, S. Alavi, P. Mayer, *Transition Met. Chem.* **2013**, 38, 267–273.
- [27] V. K. Singh, A. Maurya, N. Kesharwani, P. Kachhap, S. Kumari, A. K. Mahato, V. K. Mishra & C. Haldar. *J. Coord. Chem.* **2018**, 71, 520–541.

- [28] R. Bikas, M. Ghorbanloo, S. Jafari, V. Eigner, M. Dusek *Inorg. Chim. Acta* **2016**, *453*, 78–85.
- [29] P. M. Anarjan, R. Bikas, H. H. Monfared, P. Aleshkevych, P. Mayer, *J. of Mol. Struct.* **2017**, *1131*, 258-265.
- [30] J. Rahchamani, M. Behzad, A. Bezaatpour, V. Jahed, G. Dutkiewicz, M. Kubicki, M. Salehi, *Polyhedron* **2011**, *30*, 2611-2618.
- [31] T. S. M. Oliveira, A. C. Gomes, A. D. Lopes, J. P. Lourenço, F. A. A. Paz, M. Pillinger and I. S. Goncalves, *Dalton Trans.* **2015**, *44*, 14139.
- [32] R. Mayilmurugan, P. Traar, J. A. Schachner, M. Volpe, and N. C. M. Zanetti, *Eur. J. Inorg. Chem.* **2013**, 3664–3670.
- [33] P. Neves, L. S. Nogueira, A. C. Gomes, T. S. M. Oliveira, A. D. Lopes, A. A. Valente, I. S. Gonçalves, M. Pillinger, *Eur. J. Inorg. Chem.* **2017**, 2617–2627.
- [34] A. B. Lysenko, G. A. Senchyk, K. V. Domasevitch, M. Kobalz, H. Krautscheid, J. Cichos, M. Karbowski, P. Neves, A. A. Valente, and I. S. Goncalves, *Inorg. Chem.* **2017**, *56*, 4380–4394.
- [35] T. R. Amarante, P. Neves, F. A. A. Paz, M. Pillinger, A. A. Valente, I. S. Gonçalves, *Inorg. Chem. Commun.* **2012**, *20*, 147–152.
- [36] M. M. Antunes, T. R. Amarante, A. A. Valente, F. A. A. Paz, I. S. Goncalves and M. Pillinger, *chemCatChem* **2018**, *10*, 2782 – 2791.
- [37] M. R. Maurya, R. Tomar, L. Rana and F. Avecilla, *Eur. J. Inorg. Chem.* **2018**, 2952–2964.
- [38] T. R. Amarante, P. Neves, A. C. Gomes, M. M. Nolasco, P. R. Claro, A. C. Coelho, A. A. Valente, F. A. A. Paz, S. Smeets, L. B. McCusker, M. Pillinger, I. S. Gonçalves, *Inorg. Chem.* **2014**, *53*, 2652–2665.
- [39] a) B.S. Lane, M. Vogt, V. J. DeRose, and K. Burgess *J. Am. Chem. Soc.* **2002**, *124*, 11946-11954; b) D.E. Richardson, H. Yao, K.M. Frank, D.A. Bennett *J. Am. Chem. Soc.* **2000**, *122*, 1729-1739; c) S. K. Maiti, S. Dinda, S. Banerjee, A.K. Mukherjee, R. Bhattacharyya, *Eur. J. Inorg. Chem.* **2008**, 2038-2051; d) A. Adam; M. Mehta, *Angew. Chem., Int. Ed.* **1998**, *37*, 1387-1388 (*Angew. Chem.* **1998**, *110*, 1457-1459); e) M. Bagherzadeh, M. Aminia, H. Parastar, M. J. Heravi, A. Ellern, L. K. Woo, *Inorg. Chem. Commun.* **2012**, *20*, 86-89.
- [40] V. Conte, F. D. Furia and S. More, *Inorg. Chim. Acta* **1998**, *272*, 62–67.

- [41] C. Slebodnick and V. L. Pecoraro, *Inorg. Chim. Acta* **1998**, 283, 37–43.
- [42] R. A. Rowe, M. M. Jones, *Inorg. Synth.* **1957**, 5, 113–116.
- [43] G. M. Sheldrick, *SADABS*, version 2.10, University of Göttingen, Germany, **2004**.
- [44] G. M. Sheldrick, *SHELX*, *Acta Crystallogr., Sect. C*: **2015**, 71, 3–8.